Calcite-Dolomite Mapping to Assess Dolomitization Patterns Using Laboratory Spectra and Hyperspectral Remote Sensing: A Case Study of Bédarieux Mining Area, SE France

Nasrullah Zaini

March, 2009

Course Title:	Geo-Information Science and Earth Observation for Environmental Modelling and Management
Level:	Master of Science (Msc)
Course Duration:	September 2007 - March 2009
Consortium partners:	University of Southampton (UK) Lund University (Sweden) University of Warsaw (Poland) International Institute for Geo-Information Science and Earth Observation (ITC) (The Netherlands)
GEM thesis number:	2007-28

Calcite-Dolomite Mapping to Assess Dolomitization Patterns Using Laboratory Spectra and Hyperspectral Remote Sensing: A Case Study of Bédarieux Mining Area, SE France

by

Nasrullah Zaini

Thesis submitted to the International Institute for Geo-information Science and Earth Observation in partial fulfilment of the requirements for the degree of Master of Science in Geo-information Science and Earth Observation for Environmental Modelling and Management

Thesis Assessment Board

Chairman:	Prof. Dr. Andrew Skidmore
External Examiner:	Prof. Dr. Kasia Dabrowska-Zielinkska
Internal Examiner:	Drs. Boudewijn Desmeth
First Supervisor:	Prof. Dr. Freek van der Meer
Second Supervisor:	Dr. Harald van der Werff

ITC International Institute for Geo-Information Science and Earth Observation
Enschede, The Netherlands

Disclaimer

This document describes work undertaken as part of a programme of study at the International Institute for Geo-information Science and Earth Observation. All views and opinions expressed therein remain the sole responsibility of the author, and do not necessarily represent those of the institute.

Abstract

Reflectance spectra in the shortwave infrared (SWIR) and thermal infrared (TIR) (1.0-15 μm) contain a number of diagnostic absorption features which can be used for identification of pure and mixture of calcite and dolomite in order to characterise calcite-dolomite ratio as a proxy for assessing dolomitization patterns. The calcite-dolomite ratio were derived from laboratory reflectance spectra of synthetic samples of calcite and dolomite mixtures as a function of grain size fractions with diameter 45-500 μm, packing models from loose to compact packing sample, and mineral contents with five different weight percentage of calcite contents. The diagnostic absorption features of calcite and dolomite could be identified by the occurrences of strong vibrational absorption band positions centred at 2.34 μm and 2.5365 for pure calcite and at 2.32138 μm and 2.51485 μm for pure dolomite, while the diagnostic positions of absorption band of the calcite and dolomite in the TIR varied considerably with grain size fractions centred at 11.45–11.75 μm and 14.00–13.92 μm for pure calcite and at 11.42–11.67 μm and 13.65–13.44 μm for pure dolomite. The Positions of absorption band of the calcite and dolomite mixtures reflectance spectra in the SWIR and TIR were determined by the amount of calcite and dolomite composing the sample with calcite-dolomite ratio in the range of 2.32-2.34 μm and 2.51-2.54 μm from pure dolomite to pure calcite in the SWIR region. The ratios showed that positions of carbonate absorption band are nearly linear to the calcite content in the sample and these ratios can be used as a preliminary proxy for assessing dolomitization patterns. The diagnostic absorption features of the field samples experiment in the SWIR indicated that the majority of the field samples collected in the area between Bédarieux and Mourèze, southeastern France are dolomite and a few of rocks are calcite-dolomite mixture. A combination of laboratory spectra and hyperspectral remote sensing imagery could be used to map calcite and dolomite in order to assess dolomitization patterns in the Bédarieux mining area, southeastern France. The continuum removal spectrum of carbonate feature derived from the HyMap2003 images has been used for mapping calcite and dolomite using simple linear interpolation method. The results of calcite-dolomite mapping of the HyMap2003 images represented that the majority of abundance rocks or minerals in the study area are dominated by dolomite and the HyMap airborne hyperspectral data were fairly accurate to identify dolomite, but less accurate or sensitive to map calcite and dolomite mixtures. The dolomitization patterns in the study area were weakly identified by the HyMap images as compare to the laboratory reflectance spectra of the field samples, but the simple linear interpolation method based on spectral absorption feature parameters revealed a greatly potential to map calcite and dolomite.

Acknowledgements

In the Name of Allah, the Most Gracious, the Most Merciful

Alhamdulillah, all the praise and thanks be to Allah, the Almighty who gave me the ability to successfully complete this study.

I would like to thank the British Universities Scholarship Scheme for Higher Education Institution in Aceh and the University of Southampton, UK for awarding me the fellowship to pursue such a great opportunity course in Erasmus Mundus MSc Programme in Geo-information Science and Earth Observation for Environmental Modelling and Management (GEM).

I am all full of admiration and gratitude to my supervisor Prof. Dr. Freek van der Meer and Dr. Harald van der Werff who kindly and patiently guides and supports me with his knowledge to accomplish this research.

My sincere thank to the four coordinators of the programme: Prof. P.M Atkinson, University of Southampton; Prof. P. Pilesjö, Lund University; Prof. Katarzyna Dabrowska, University of Warsaw and Prof. A. Skidmore, ITC. I am really grateful to them and Mr. Andre Kooiman as course coordinator for their continuous guidance and support during the study.

I would like to express my gratitude to all the teachers of four institutions for their valuable knowledge and also to the Ms. Stephanie Webb and Ms. Jorien Terlouw for their help with information and logistics.

I am grateful to Drs. Boudewijn de Smeth and C.A Hecker, M.Sc for their help and assistance during laboratory work and my special thank to Prof. S.M de Jong, Utrecht University for his help to collect field samples.

I would like to thank Syiah Kuala University, Banda Aceh for granting me to study abroad and my humble appreciation to all my fellow classmates and Indonesian students in ITC who support me during the study.

Finally my deepest gratitude to my parents Zaini Usman and Cut Nilawati Ibrahim, my wife Cut Juwairiah Djuned, my beloved daughter Iffatun Nisa Nasrullah, and my sisters Mukhsanati and Nurul Aida who have always supported and inspired me to strive for higher quality of life.

Table of contents

List of figures

List of tables

1. Introduction

1.1. Background and Significance

Dolomitization is an alteration process of limestone into dolomite by replacing calcite with dolomite which marks an increase in the porosity of the rock by 12 % that makes it more suitable for oil reservoirs (Harbaugh, 1967; Van der Meer, 1994; 1995). This process involves the replacement of calcite (calcium carbonate, $CaCO_3$) by dolomite (calcium magnesium carbonate, $CaMg(CO_3)_2$) in the rock when magnesium-rich water permeates through limestone (Deffeyes *et al*, 1964; Hatch and Rastall, 1965; Friedman and Sanders, 1967).

Limestone or carbonate rocks are sedimentary rocks and metamorphic rocks that are mostly formed by calcite and dolomite. These carbonate minerals occur as trigonal crystal systems and are usually white in colour. Even though the physical properties of dolomite are almost same as calcite, dolomite rarely forms more complex crystals and is simple rhombohedral in shape (Hatch and Rastall, 1965; Bissell and Chilingar, 1967; Hunt and Salisbury, 1971; Kirkaldy, 1976; Dietrich and Skinner, 1979; Hamilton *et al*, 1995). Calcite and dolomite, in the form of limestone, are important to industry being used extensively in construction materials and essential in the making of cement (Dietrich and Skinner, 1979; Hamilton *et al*, 1995).

Moreover, the carbonate minerals also have an important economic value in terms of petroleum geology due to the dolomitization process (Harbaugh, 1967; Van der Meer, 1994; 1995). The substitution process of the minerals by other minerals, for instance calc-silicates consisted of garnet and pyroxene will probably produce granitic rocks and skarns which are a source of valuable mineral deposits such as copper, gold, iron, lead, zinc, or tungsten (Van der Meer, 1994; 1995). The positive impact of dolomitization patterns on oil explorations and the source of valuable mineral deposits make it a more favourable mineral to be investigated using remote sensing technology.

Airborne hyperspectral remote sensing imagery, which consists of many images, with narrow and contiguous spectral bands, have been widely used for geological explorations, especially for identifying and mapping earth surface minerals in many areas around the world. Several studies of mineralogy mapping using airborne

hyperspectral remote sensing imagery have been conducted by numerous authors (Bierwirth *et al*., 2002; Kratt *et al*, 2006; Riaza *et al*., 2005; Van der Meer, 2004, 2006a, 2006b; Van Ruitenbeek *et al.*, 2006; 2008). A study by Choe *et al*. (2008) showed that field spectroscopy and hyperspectral remote sensing can be applied to map the mineral surface of heavy metal pollution in the Rodalquilar mining area, southeastern Spain. Windeler and Lyon (1991) revealed that calcite can be distinguished from dolomite based on specific spectral reflectance in near infrared through laboratory experiment and remote sensing. The work of Van der Meer (1994) reported that a combination between calcite and dolomite mixtures in laboratory spectra and high-spectral resolution remote sensing imagery enabled to map dolomitization patterns in the Igualeja-Istán area, southern Spain. Therefore, hyperspectral remote sensing data of calcite and dolomite mapping is one of the possible methods that can be applied in assessing dolomitization patterns.

The development of more sophisticated spectroscopy technology has created a possibility to characterize spectral features of minerals not only in the shortwave infrared (SWIR) but also in the thermal infrared (TIR). Carbonate minerals have diagnostic absorption features of reflectance spectra in the SWIR and TIR band due to electronic and vibrational processes, so that the spectra can be used to discriminate carbonate minerals from other minerals and identify calcite and dolomite with another carbonate minerals (Hunt and Salisbury, 1971; Gaffey, 1985; 1986; Crowley, 1986; Van der Meer, 1994; 1995; 2004; 2006c; Clark, 1999; Gupta, 2003). Van der Meer (1995) stated that estimation of the calcite-dolomite ratio from spectra could be done using diagnostic absorption features in the SWIR around 2.30-2.34 μm, of which the exact position is dependent on the amount of calcite versus dolomite. Furthermore, Van der Meer (1994, 1995) found a near linear relationship between the calcite-dolomite ratio and the position of the carbonate absorption feature, however that was determined using a synthetic data set. In a study of calcite and dolomite absorption features in the TIR region, Huang and Kerr (1960) indicated that calcite and dolomite have a strong position of absorption wavelength at 11.40 μm and 11.35 μm respectively. Recently, Reig *et al*. (2002) has drawn attention to the fact that Fourier Transform Infrared (FTIR) spectroscopy could be used to determine the position of absorption wavelength for calcite at 875 and 712 cm^{-1} or 11.43 and 14.04 μm and the position of absorption wavelength for dolomite at 881 and 730 cm^{-1} or 11.35 and 13.70 μm. So mapping of calcite and dolomite in order to assess dolomitization patterns using laboratory spectra in the SWIR and TIR region and hyperspectral remote sensing data in the Bédarieux mining area, southeastern France would be a necessary and interesting topic to be undertaken.

1.2. Research Problem

Although some research has identified and mapped surface minerals using the HyMap (Hyperspectral Mapper) airborne hyperspectral remote sensing data, research has yet to be conducted for mapping calcite and dolomite in the Bédarieux mining area, southeastern France. A previous study mapped calcite and dolomite mixtures to assess dolomitization patterns using high-spectral resolution remote sensing imagery (GERIS) in southern Spain (Van der Meer, 1994). Hyperspectral technology contains many images, with narrow and contiguous spectral bands, and this could be a more precise method to detect the spectral reflectance characteristics of calcite and dolomite. It may, however, have several problems in the identification of calcite and dolomite mixtures' spectra, which is a proxy for assessing dolomitization patterns in the study area. This may be due to the limitations of spectral and spatial resolution as compared to the laboratory spectra.

In addition, the position of calcite and dolomite absorption features in the SWIR and the TIR have been observed by many researchers, but the precise position of absorption band of these minerals have been at significantly different wavelengths (Huang and Kerr, 1960; Hunt and Salisbury, 1971; Gaffey, 1985; 1986; Van der Meer, 1994; 1995; Reig *et al*., 2002). The reason could be the different spectral resolution of the spectroscopy instruments used for measuring the minerals reflectance spectra. These absorption features of reflectance spectra of calcite and dolomite might also be influenced by various physical and chemical parameters such as grain size fractions (Crowley, 1986; Gaffey, 1986; Salisbury *et al*., 1987; Van der Meer, 1994; 1995; Clark, 1999), packing or porosity (Gaffey, 1986), and mineral contents or mineral mixtures (Gaffey, 1985; Salisbury *et al*., 1987; Van der Meer, 1994; 1995; Clark, 1999). So a new research approach using a sophisticated spectrometer and the HyMap data is essential.

1.3. Research Objective

The research objective of this study is divided into two parts, namely general objective and specific objective.

1.3.1. General Objective

The general objective of the research is to estimate the calcite-dolomite ratio for assessing dolomitization patterns in the Bédarieux mining area, southeastern France and to determine the reflectance spectra association of calcite and dolomite between laboratory spectra and airborne hyperspectral remote sensing imagery.

1.3.2. Specific Objectives

The specific objectives of the research are:

- to characterize the absorption features of the pure powdered moura calcite marble and chemical pure dolomite reflectance spectra in the SWIR and TIR region based on synthetic samples in order to identify changes of spectral characteristic as a function of grain size fractions, packing models, and mineral contents.
- to identify the diagnostic absorption features of the carbonate rock samples reflectance spectra in the SWIR collected from the area between Bédarieux and Mourèze, southeastern France.
- to determine which reflectance spectra can visually identify the calcite-dolomite ratio in order to assess dolomitization patterns on the study area using the HyMap airborne hyperspectral remote sensing data.
- to validate the reflectance spectra of calcite and dolomite used as a preliminary proxy for assessing dolomitization patterns of the synthetic samples, and the HyMap data with field samples.

1.4. Research Questions

- Do the differences in grain size fractions, packing models, and mineral contents of the pure powdered moura calcite marble and chemical pure dolomite of the synthetic samples influence the absorption features of the carbonate minerals reflectance spectra in the SWIR and TIR region?
- Do the absorption features of spectral reflectance characteristics of the rock samples from the study area in the SWIR region indicate pure calcite and dolomite or calcite-dolomite mixtures?
- Can the HyMap airborne hyperspectral remote sensing imagery identify calcite and dolomite reflectance spectra which are a proxy for assessing dolomitization pattern on the study area?
- To what degree of accuracy can we detect dolomitization patterns in the study area using the HyMap airborne hyperspectral data as compared to the laboratory reflectance spectra of the synthetic samples and field samples?

1.5. Hypotheses

- The differences in grain size fractions, packing models, and mineral contents of the pure powdered moura calcite marble and chemical pure dolomite of the synthetic samples influence the absorption features of the carbonate minerals reflectance spectra in the SWIR and TIR region.

- The absorption features of spectral reflectance characteristics of the rock samples from the study area in the SWIR region indicate a pure dolomite and calcite-dolomite mixtures.
- The HyMap airborne hyperspectral remote sensing imagery can identify calcite and dolomite reflectance spectra which are a proxy for assessing dolomitization pattern on the study area.
- The HyMap airborne hyperspectral data can detect dolomitization patterns on the study area at a certain degree of accuracy as compared to the laboratory reflectance spectra of the synthetic samples and field samples.

1.6. Research Approach and Thesis Structure

The research has been conducted as an integrated process that involved literature review, laboratory experiments of synthetic and field samples, absorption features analysis of synthetic and field samples' reflectance spectra, and processing of the hyperspectral imagery.

The synthetic samples experiment was performed strictly through a series of procedures and stages, namely sample preparation: pulverising of the rock samples of moura calcite marble and chemical pure dolomite and sieving of the powdered minerals into six different grain size fractions with a diameter between 45 μm and 500 μm, packing of the samples with different compactness models, and mixing of the calcite and dolomite with different mineral contents and grain size fractions; spectral measurement of the pure and mixture of synthetic samples in the SWIR and TIR band; and spectral data analysis.

The field samples experiment was accomplished through the following processes: field samples collection in the area between Bédarieux and Mourèze, the Hérault department of Languedoc-Roussillon region, southeastern France; sample preparation in order to obtain a fresh and flat rock surface with a diameter at least 3 cm, spectral measurement of the samples in the SWIR, and spectral data analysis.

In the final stage, the HyMap airborne hyperspecral remote sensing imagery was processed through several steps: vegetation masking using a Normalized Difference Vegetation Index (NDVI); continuum removed images at certain wavelengths that indicate the diagnostic absorption features of the carbonate minerals; reflectance spectra analysis; calcite and dolomite mapping for assessing dolomitization patterns using "a simple linear interpolation method" based on the work of Van der Meer (2004, 2006b); and validation.

2. Literature Review

2.1. Carbonate Minerals

Carbonate rocks or limestone are sedimentary rocks and metamorphic rocks that are mostly formed by calcite (calcium carbonate, $CaCO_3$) and dolomite (calcium magnesium carbonate, $CaMg(CO_3)_2$). In the nature, carbonate minerals can also be found in another various types such as siderite ($FeCO_3$), magnesite ($MgCO_3$), aragonite ($CaCO_3$), ankerite $CaFe(CO_3)_2$, rhodochrosite ($MnCO_3$), strontianite ($SrCO_3$), cerussite ($PbCO_3$), witherite ($BaCO_3$), malachite ($Cu_2CO_3(OH)_2$), and azurite ($Cu_3(CO_3)_2(OH)_2$) (Hatch and Rastall, 1965; Bissell and Chilingar, 1967; Hunt and Salisbury, 1971; Kirkaldy, 1976; Dietrich and Skinner, 1979; Hamilton *et al*, 1995). However, the main focus of discussion in this section is only to explain the two essential carbonate minerals forming the rocks, calcite and dolomite, and its alteration process in the carbonate rocks called dolomitization (Deffeyes *et al*, 1964; Hatch and Rastall, 1965; Friedman and Sanders, 1967).

2.1.1. Calcite

Calcite, a stable compound of calcium carbonate, is a common mineral found in limestone (calcareous sedimentary rocks), igneous rocks and metamorphic rocks. The mineral occurs as trigonal crystal system and the crystal shapes are well distributed and perfect. In addition, another carbonate mineral having identical chemical composition to calcite is aragonite, but the crystal system of the mineral is orthorhombic. Calcite has a wide variety of colours in its appearance which is usually colourless or white and shaded by grey and black due to the presence of organic matter, yellowish, brown or reddish due to iron oxides impurity, greenish due to infiltrating of clayey mineral into the rock, purple, and blue. The mineral can also be distinguished from other minerals by its specific characteristics for instance perfect rhombohedral cleavage, dissolving quickly in cold dilute hydrochloric acid and its presence is assigned by effervescence, and the hardness value is 3, consequently it is easy to pulverise into a powder with different grain size fractions (Hatch and Rastall, 1965; Bissell and Chilingar, 1967; Hunt and Salisbury, 1971; Kirkaldy, 1976; Dietrich and Skinner, 1979; Hamilton *et al*, 1995). In economic point of view, calcite in the form of limestone has been used widely as construction material, mortar and cement, fertilizer, and flux for smelting of iron ores (Dietrich and Skinner, 1979; Hamilton *et al*, 1995). Dietrich and Skinner (1979) have drawn

attention to the fact that calcite is also used in pharmaceutical materials for example as a medicine for neutralising of stomach acids.

2.1.2. Dolomite

Dolomite is an important mineral composing many sedimentary rocks, dolomitic limestone and consists of a calcium magnesium carbonate. In weight percentage, pure dolomite mineral is formed by 45.7% $MgCO_3$ and 54.3% $CaCO_3$ or 47.8% CO_2, 21.8% MgO, and 30.4% CaO. The physical properties of dolomite are almost same as calcite, so it is relatively difficult to differentiate between the two carbonate minerals. The mineral occurs as trigonal crystal system but dolomite rarely forms more complex crystals and is simple rhombohedral. Dolomite also has various colours in its appearance which is generally white and sometime it may be reddish, brown, greenish, gray or black due to infiltrating of other matters into the rock. In contrast to the calcite, dolomite dissolves pathetically in cold dilute hydrochloric acid and it effervesces if the mineral is immersed in a warm hydrochloric acid, and the hardness value is between 3.5 and 4, therefore it is still fairly easy to pulverise into a powder with different grain size fractions (Hatch and Rastall, 1965; Bissell and Chilingar, 1967; Hunt and Salisbury, 1971; Kirkaldy, 1976; Dietrich and Skinner, 1979; Hamilton *et al*, 1995). Dolomite has a valuable economic perspective on industrial era, because it is extensively used as construction materials, aggregate for making of cement, and source of magnesium extraction for refractory bricks (Dietrich and Skinner, 1979; Hamilton *et al*, 1995).

2.1.3. Dolomitization

The phenomena of dolomitization in limestone have been discussed by many authors (Deffeyes *et al*, 1964; Berner, 1965; Hatch and Rastall, 1965; Friedman and Sanders, 1967). Dolomitization is an alteration process of limestone into dolomite by replacing calcite with dolomite which marks an increase in the porosity of the rock by 12 % that makes it more suitable for oil reservoir (Harbaugh, 1967; Van der Meer, 1994; 1995). This process involves the replacement of calcite ($CaCO_3$) by dolomite ($CaMg(CO_3)_2$) in the rock when magnesium-rich water permeates through limestone (Deffeyes *et al*, 1964; Hatch and Rastall, 1965; Friedman and Sanders, 1967). A study by Harbaugh (1967) points out that the chemical reaction of the alteration process by replacing calcite with dolomite such as when calcite reacts with magnesium chloride is provided by:

$$2\ CaCO_3 + MgCl_2 \longrightarrow CaMg(CO_3)_2 + CaCl_2$$

Harbaugh also concluded that the replacement of calcite by dolomite in the limestone might be happened on "the basis of a molecule-by-molecule or a volume-by-volume" and the amount of dolomite in the rock will influence the level of porosity.

Moreover, the carbonate minerals have an important economic value in term of petroleum geology due to dolomitization process (Harbaugh, 1967; Van der Meer, 1994; 1995) and the substitution process of carbonate minerals by other minerals for instance calc-silicates that are consisted of garnet and pyroxene will probably produce granitic rocks and skarns which are a source of valuable mineral deposits such as copper, gold, iron, lead, zinc, or tungsten (Van der Meer, 1994; 1995). The positive impact of dolomitization patterns on oil explorations and the source of valuable mineral deposits make it more favourable minerals to be investigated using remote sensing technology.

2.2. Spectra of Carbonate Minerals

The electromagnetic radiation that contain and propagate a number of energy will have a series of physical or optical processes such as absorption, reflection, and transmission when the radiations interact with minerals or rocks on the earth surface. Each feature or mineral has a unique response in interaction with electromagnetic radiation, and it will create a diagnostic spectral signature or spectral response curve (Campbell, 1996; Clark, 1999; Gupta, 2003). The spectra convey a unique of information related to a particular mineral or substance forming the rock. Carbonate minerals, an essential mineral on the earth surface, also have a diagnostic spectral signature or spectral feature, as a result of its interaction with electromagnetic radiation, so that it can be distinguished from other minerals (Huang and Kerr, 1960; Hunt and Salisbury, 1971; Gaffey, 1985; 1986; 1987; Crowley, 1986; Van der Meer, 1994; 1995; 2006c; Clark, 1999; Gupta, 2003). In this section, the primary discussion is based on literature review of those authors which is focused on spectral features of carbonate minerals and its interactions with electromagnetic radiation.

2.2.1. Fundamental Concepts of Spectroscopy

The basic principle of spectroscopy is derived from the interactions of electromagnetic radiation with materials which are a solid, liquid, or gas. The interactions will generate a series of physical or optical process such as absorption, reflection, and transmission that contain certain information of the materials or minerals. Campbell (1996) and Clark (1999) revealed that spectroscopy is the study of the interaction between electromagnetic radiation and materials which results

spectra of the materials at specific wavelengths. When the electromagnetic radiation or light, which are referred to photons or package of energy, penetrate a mineral or rock, so part of its energy are reflected by grain surfaces, some are absorbed by the grain or substance composing the rock, and part of its energy are transmitted through the grain or matters at particular wavelengths. The reflected energy from the grain surface of the mineral could be measured or recorded by various instruments for instance spectrometer. Reflectance is the ratio of the energy or intensity of light reflected from a surface of material or mineral to the intensity of the light incident on it. The spectrometer measuring reflectance is called reflection or reflectance spectrometer which is an integrated system including a light source, an optical system such as prism to disperse polychromatic light into monochromatic light, and a detector that measures the intensity of reflected light (Gaffey, 1985; Van der Meer, 1995; 2006c; Clark, 1999; Gupta, 2003). The absorptions of electromagnetic energy at particular wavelengths in minerals or rocks are caused by several processes such as electronic and vibrational processes (Hunt and Salisbury, 1971; Hunt, 1977; Gaffey, 1985; Van der Meer, 1994; 1995; 2004; 2006c; Gaffey *et al*., 1997; Clark, 1999; Gupta, 2003).

2.2.2. Electronic Processes in the Visible and Near Infrared Band

Absorption features of minerals or rocks in visible and near infrared (VNIR) region are determined by electronic processes or transitions which involve a number of processes in electronic or atomic level for instance crystal field effect, charge transfer effect, and conduction band effect. Crystal field effect, which is caused by incompletely filled electron shells of transition elements such as Ni, Cr, Co, Fe, and Mn, is a dominant electronic process of absorption features of minerals. These transition elements have different energy level when it is situated in different crystal fields. An energetic electron due to absorption of photons, which is isolated at a particular crystal field, would be able to pass its energy gap from the lower to higher energy level. Therefore, the mineral diagnostic absorption bands of crystal field effect differ from other minerals and depend on valence state, coordination number, site symmetry, type of ligand, lattice distortion, and the distance between metal and ligand. Moreover, the absorption features due to charge transfer effect occur in electronic scale or inter-element transitions. When photons interact with minerals, a part of the energy is absorbed by electrons so the electron has enough energy for moving between neighbouring metal ions, called charge transfer effect. A common charge transfer effect occurs between iron ions such as ferrous (Fe^{2+}) and ferric (Fe^{3+}) and it determines diagnostic spectral features of the mineral. The presence of iron oxides (Fe-O) in minerals is assigned by a red colour due to charge transfer

absorptions. Conduction band effect also influence absorption features in visible and near infrared band where the difference in energy level between conduction band and valence band will affect absorption bands, especially in semiconductor materials (Hunt and Salisbury, 1971; Gaffey, 1985; 1986; Van der Meer, 1994; 1995; 2004; 2006c; Gaffey *et al*., 1997; Clark, 1999; Gupta, 2003). Hunt and Salisbury (1971) concluded that the absorption features of carbonate spectra in visible and near infrared region are caused by electronic processes in metal cations or impurity ions, or its interaction in crystal field.

2.2.3. Vibrational Processes in the SWIR and TIR Band

Theoretically the studies of minerals forming the rock using absorption features of reflectance spectra in the shortwave infrared (SWIR) band have been conducted by several authors (Huang and Kerr, 1960; Hunt and Salisbury, 1971; Hunt, 1977; Hunt, 1982; Gaffey, 1985; 1986; 1987; Crowley, 1986; Van der Meer, 1994; 1995; 2004; 2006c; Gaffey *et al*., 1997; Clark, 1999; Gupta, 2003). They revealed that the absorption features of minerals spectra at a particular position in the SWIR region, which are the result of vibrational processes, are caused by the occurrence of hydroxyl ion (OH^-), water molecule (H_2O), carbonate, and other minerals. The vibrational absorptions in molecule scale consist of three modes of vibrations such as fundamental, overtone, and combination. Those authors described that the identical absorption feature around 1.4 μm is affected by overtone of hydroxyl ion and when the hydroxyl stretches exist in combination with water molecule, the absorption feature is occurred at about 1.9 μm. The strong vibrational absorption features can be seen in the range 2.2-2.3 μm due to interaction between hydroxyl and metal ions such as Al and Mg forming a bonding as Al-OH (Aluminium Hydroxide) and Mg-OH (Magnesium Hydroxide) and the presence of clay mineral in the rock can be identified in the range 2.1-2.4 μm.

Carbonates minerals have a more precise and sharp vibrational absorption features at 2.30-2.35 μm and 2.50-2.55 μm due to CO_3^{-2} ion. It is the diagnostic absorption features of carbonates minerals and the positions of absorption band are determined by the purity level and composition of the minerals. Hunt and Salisbury (1971), Gaffey (1985, 1986, 1987), Van der Meer (1994, 1995, 2004, 2006c), and Clark (1999) observed that the additional carbonate vibrational bands occur around 2.12-2.16 μm, 1.97-2.00 μm, and 1.85-1.87 μm. Gaffey (1985, 1986, 1987) also founded two weaker absorption carbonate bands at 2.23-2.27 μm and 1.75-1.80 μm. Salisbury *et al*. (1987) reported that the carbonate ion have absorption bands in the wavelength range from 1500 cm^{-1} to 650 cm^{-1} (6.67-15.38 μm) due to strong

fundamental molecular vibrations, a stretching vibrational absorption around 1425 cm^{-1} (7.02 μm) and two bending vibrational absorptions at about 875 cm^{-1} and 700 cm^{-1} (11.43 μm and 14.28 μm). Furthermore, Hunt (1982), Clark (1999), and Gupta (2003) stated that absorption features of minerals or rocks in the thermal infrared (TIR) are caused by vibrational processes of asymmetry and asymmetry stretching of Si-O-Si, O-Si-O, H-O-Al, Fe-O, and Al-O.

2.2.4. Spectral Features of Carbonate Minerals in the SWIR and TIR Band

Carbonate minerals have diagnostic absorption features of reflectance spectra in the SWIR and TIR band due to electronic and vibrational processes, as mentioned in the previous section. These spectral features have been used to discriminate carbonate minerals from other minerals and identify calcite and dolomite with another carbonate mineral on the earth surface. Furthermore, the absorption features of reflectance spectra in the visible to near infrared, which are a unique signature of each mineral, have also been used as an alternative technique of non-destructive testing to analyse mineral and chemical composition of samples or rocks rapidly (Gaffey, 1986; 1987; Van der Meer, 1995; 2006c). This section only reviewed the spectral features of the two most common carbonate minerals forming the rock such as calcite and dolomite in the SWIR and TIR region based on the work of several authors (Huang and Kerr, 1960; Hunt and Salisbury, 1971; Gaffey, 1985; 1986; 1987; Crowley, 1986; Van der Meer, 1994; 1995; Clark, 1999; Reig *et al*., 2002).

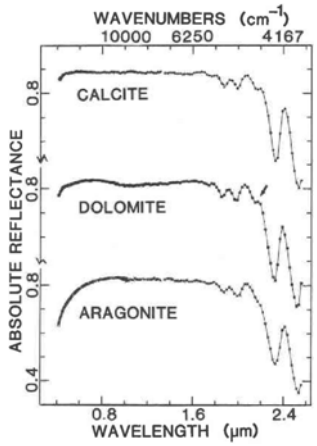

Figure 2.1. Spectral features of calcite, dolomite, and aragonite in the visible to SWIR region. A weaker absorption feature of calcite and dolomite spectra at 2.23 -2.27 μm is shown by arrow (*Source:* Gaffey, 1986: 152).

In a study of carbonates minerals absorption features in the SWIR band, Huang and Kerr (1960), Hunt and Salisbury (1971), Gaffey (1986, 1987), and Van der Meer (1994) indicated a significant difference in the precise position of calcite and dolomite absorption band, where Huang and Kerr (1960) observed that calcite is centred at 3.92 µm and dolomite is at 3.95 µm, Hunt and Salisbury (1971) found that calcite is centred at 2.35 µm and dolomite is at 2.33 µm, Gaffey (1986, 1987) reported that calcite is centred around 2.33-2.34 µm and dolomite is at about 2.31-2.32 µm, and Van der Meer (1994) concluded that calcite is centred at 2.3465 µm and dolomite is at 3.3039 µm. The absorption features of reflectance spectra of calcite, dolomite, and aragonite in the range of wavelength between visible and SWIR is depicted in Figure 2.1 (*from* Gaffey, 1986). Gaffey also revealed the precise position and width of absorption band of calcite and dolomite in the SWIR, as provided in Table 2.1.

Table 2.1. The position and width of absorption band of calcite and dolomite in the SWIR (*After:* Gaffey, 1986).

Carbonate Band	Calcite		Dolomite	
	Position (µm)	Width (µm)	Position (µm)	Width (µm)
1	2.530-2.541	0.0223-0.0255	2.503-2.518	0.0208-0.0228
2	2.333-2.340	0.0154-0.0168	2.312-2.322	0.0173-0.0201
3	2.254-2.720	0.0121-0.0149	2.234-2.248	0.0099-0.0138
4	2.167-2.179	0.0170-0.0288	2.150-2.170	0.0188-0.0310
5	1.974-1.995	0.0183-0.0330	1.971-1.979	0.0206-0.0341
6	1.871-1.885	0.0190-0.0246	1.853-1.882	0.0188-0.0261
7	1.753-1.885	0.0256-0.0430	1.735-1.740	0.0178-0.0395

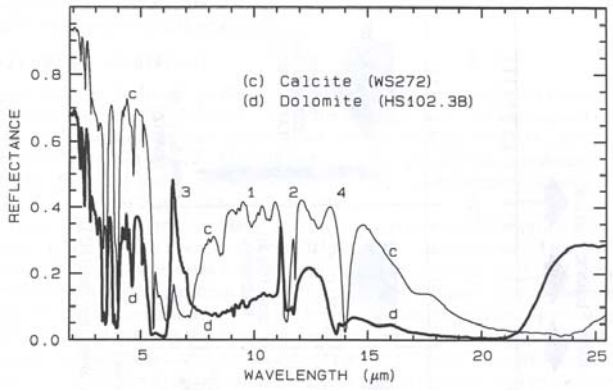

Figure 2.2. Spectral features of calcite and dolomite in the SWIR to TIR region (*Source:* Clark, 1999: 25).

The work of Huang and Kerr (1960) indicated that calcite and dolomite have a strong position of absorption band in the TIR at 11.40 μm and 11.35 μm respectively. It is the view of Clark (1999) that the position of absorption band of calcite and dolomite reflectance spectra in the TIR are slightly shifted due to different composition of the two minerals (Figure 2.2.). Reig *et al*. (2002) has drawn attention to the fact that FTIR spectroscopy could be used to determine absorption features of calcite at 875 cm^{-1} and 712 cm^{-1} or 11.43 μm and 14.04 μm and dolomite at 881 cm^{-1} and 730 cm^{-1} or 11.35 μm and 13.70 μm.

2.2.4.1. Effects of Grain Size Fractions and Mineral Contents on the Spectral Features of Calcite and Dolomite

The absorption features of reflectance spectra of calcite and dolomite or other minerals in the SWIR are influenced by various physical and chemical parameters such as grain size fractions (Crowley, 1986; Gaffey, 1986; Salisbury *et al*., 1987; Van der Meer, 1994; 1995; Clark, 1999), packing or porosity (Gaffey, 1986), mineral contents or mineral mixtures, and chemical composition (Gaffey, 1985; Salisbury *et al*., 1987; Van der Meer, 1994; 1995; Clark, 1999). In a study of grain size fractions effects on spectral features of carbonate minerals or calcite and dolomite, Crowley (1986), Gaffey (1986), Salisbury *et al*. (1987), and Van der Meer (1994, 1995) revealed that the differences in grain size fractions of calcite and dolomite influence its spectral features, especially depth of absorption band and overall brightness of the minerals in the SWIR. However, other absorption features such as position, width, and asymmetry of absorption band are invariance with grain size fractions. The depth of absorption band increase considerably with increasing grain size fractions of calcite and dolomite, whereas the overall brightness of the minerals decrease significantly with increasing grain size fractions. The grain size fractions effects on absorption features of the calcite reflectance spectra are illustrated in Figure 2.3. (a) (*from* Gaffey, 1986).

These phenomena are matched with the Lambert-Beer Law as described in the equation (2.1), where the output or attenuated intensity of electromagnetic energy, which passes through a material, is a function of thickness of the material. Clark and Roush (1984) mentioned that the coarse grain or particle size fractions of the mineral absorb more electromagnetic radiation than fine grain size fractions due to longer internal optical path and multiple interactions within the particle as a medium that will be passed by the electromagnetic radiation.

$$I = I_o e^{-kx} \tag{2.1}$$

Where I_o is the input or initial intensity of electromagnetic radiation, I is the output or attenuated intensity of electromagnetic radiation, x is thickness of material, and k is absorption coefficient. Gaffey (1986) also indicated that the absorption features of carbonate minerals reflectance spectra are determined by packing or porosity as depicted in Figure 2.3 (b) between rock and powder sample. The differences in packing or porosity of the minerals influence its spectral features, particularly depth of absorption band and overall brightness.

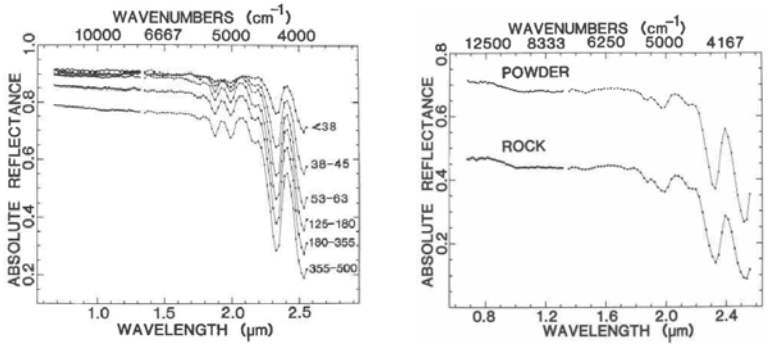

(a) (b)

Figure 2.3. Spectral reflectance of (a) powdered calcite sample (Iceland spar) with different grain size fractions and (b) powder and rock sample of dolomite with different packing or porosity in the visible to SWIR region (*Source:* Gaffey, 1986: 154).

In terms of mineral contents or mineral mixtures effects on absorption features of carbonate minerals, Van der Meer (1994, 1995) stated that absorption features of calcite and dolomite mixtures reflectance spectra are determined by the amount of calcite and dolomite composing the sample and the position of absorption band is nearly linear to calcite content of the sample (Figure 2.4). The position of absorption band of calcite and dolomite mixtures is centred in the range of 2.30 - 2.34 μm from pure dolomite to pure calcite in the sample. The work of Gaffey (1985) observed that chemical compositions in the calcite and dolomite samples also influence the position of absorption band of calcite and dolomite. Gaffey described that the dolomite positions of absorption band shift to longer wavelength when the amount of Fe increase in the sample, while the calcite positions of absorption band shift to shorter wavelength when the amount of Mg increase in the sample. In addition, Salisbury *et al*. (1987) pointed out that the presence of opaque minerals in a mineral mixture will decrease reflectance intensity of the mineral.

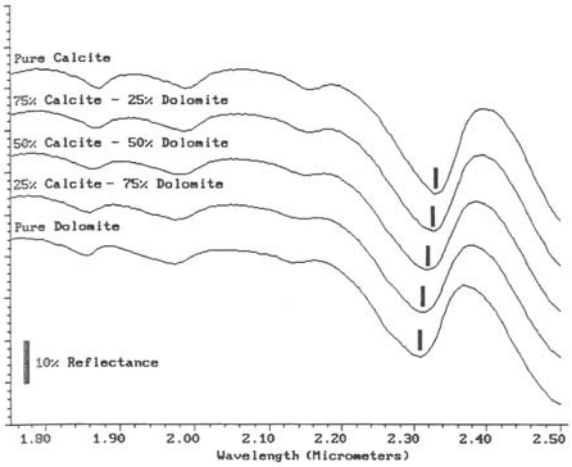

Figure 2.4. Reflectance spectra of calcite and dolomite mixture in the SWIR region (*Source:* Van der Meer, 1995: 77).

2.3. Hyperspectral Remote Sensing in Minerals Mapping

The invention and development of aerial photography and sensor technology have played an important role in remote sensing for observing and classifying a distant object or image on the earth surface. However, the technology has certain limitations to obtain specific information related to a particular earth mineral due to broad spectral band or low spectral resolution. The recent advance remote sensing technology, hyperspectral remote sensing, has allowed to acquire a precise earth surface mineralogy image due to high spectral resolution, so it can be used for identifying and mapping of a specific mineral (Goetz, 1991; Campbell, 1996; Mustard and Sunshine, 1999; Van der Meer *et al*., 2006; Sabins, 2007).

Hyperspectral remote sensing imagery, particularly airborne hyperspectral remote sensing imagery or airborne imaging spectrometer data which consists of a numerous remotely sensed data, narrow, and contiguous spectral bands, have been widely used for geological explorations, especially for identifying and mapping earth surface minerals in many areas around the world. Several studies of mineralogy mapping using airborne hyperspectral remote sensing imagery such as AVIRIS, DAIS and HyMap have been conducted by many authors (Bierwirth *et al*., 2002; Kratt *et al*, 2006; Riaza *et al*., 2005; Van der Meer, 2004; 2006a; 2006b; Van Ruitenbeek *et al.*, 2006; 2008). A study by Choe *et al*. (2008) showed that field spectroscopy and hyperspectral remote sensing can be applied to map the mineral

surface of heavy metal pollution in the Rodalquilar mining area, SE Spain. Windeler and Lyon (1991) revealed that calcite can be distinguished from dolomite based on specific spectral reflectance in near infrared through laboratory experiment and remote sensing data. The work of Van der Meer (1994) reported that a combination between calcite and dolomite mixtures laboratory spectra and high-spectral resolution remote sensing imagery (GERIS), enabled to map dolomitization patterns in the Igualeja-Istán area, southern Spain. Therefore, the hyperspectral remote sensing data in calcite and dolomite mapping is one of the possible methods that can be applied in assessing dolomitization patterns.

2.3.1. Hyperspectral Mapper (HyMap)

"HyMap" (Hyperspectral Mapper), a whiskbroom scanning instrument, was designed by Integrated Spectronics Pty Ltd, Australia and operated by HyVista Corporation to acquire 126 channels of data in the visible, near infrared, and shortwave infrared that cover the wavelength range from 0.45 to 2.5 μm, excluding atmospheric water absorption bands near 1.4 and 1.9 μm. This instrument, that has spatial resolution between 2 and 10 m per pixel and at approximately 15 nm spectral resolutions, is carried aboard the twin-engine aircraft at altitudes between 2000 and 5000 m above ground level (Cocks *et al*., 1998, Van der Meer *et al*., 2006). The hyperspectral imagery is the three-dimensional *data cube*, where x axis represents wavelength, y axis represents reflectance or brightness, and z axis represents the accumulation of spectral bands (Campbell, 1996; Van der Meer *et al*., 2006). The detail operating system and configuration specifications of the imaging spectrometer are provided in the Appendix I.

2.3.2. Hyperspectral Data Processing and Mapping Approach

In this section, the literature review focused on processing and mapping approach of hyperspectral remote sensing data using absorption features of reflectance spectra analysis and "a simple linear interpolation method" based on the work of Van der Meer (1995, 2004, 2006b) and Van der Meer *et al*. (2006). These absorption features, which are used for processing and mapping approach of hyperspectral data, are derived from the continuum removed spectral reflectance as observed by Clark and Roush (1984). Van der Meer (1995, 2004) stated that the absorption features of a reflectance spectrum consist of two main parameters such as a continuum and individual features, where continuum or background is a convex hull of straight-line segments put on the overall maximum pixel of reflectance spectrum in order to derive the ratio between the reflectance spectrum and the convex hull line segments. After that the continuum removal spectra, which are acquired from both laboratory

spectrometer and airborne imaging spectrometer, can be used to calculate absorption feature parameters such as position or centre of absorption band, depth of absorption band, width of absorption band, and asymmetry of absorption band.

The position of absorption band, λ, is defined as the wavelength where the position of maximum absorption or minimum reflectance of an absorption feature occurred (Van der Meer, 1995, 2004; Van der Meer *et al*., 2006). The depth, *D*, of the absorption feature indicates the reflectance value at the shoulders minus the ratio of reflectance value at the position of absorption wavelength, R_b is the reflectance at the band bottom and R_c is the reflectance of the continuum at the same band as R_b. (Clark and Roush, 1984; Van der Meer, 2004). The depth of absorption band of the spectral feature is described by the following formula (Clark and Roush, 1984; Van der Meer, 2004).

$$D = 1 - \frac{R_b}{R_c} \tag{2.2}$$

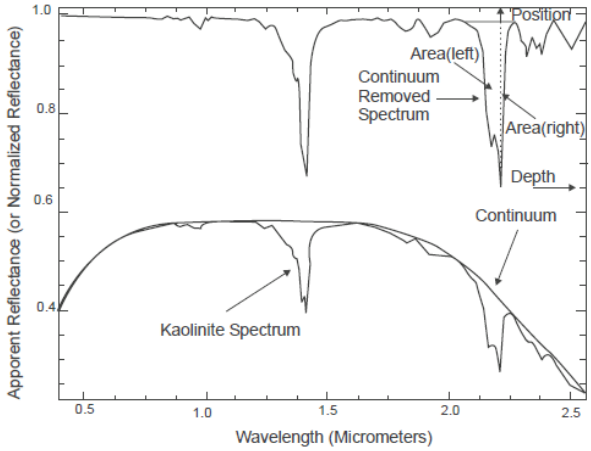

Figure 2.5. Continuum and continuum removal process to enhance absorption feature characteristics of reflectance spectra (*Source:* Van der Meer, 2004: 57).

The width of an absorption feature between left shoulder and right shoulder of the feature is defined as the sum of the area left (A_{left}) of absorption position and the area right (A_{right}) of absorption position and divided by two times the depth value of the feature (Van der Meer, 1995; Van der Meer *et al*., 2006). The width of absorption feature, *Width*, is formulated as

$$Width = \frac{(A_{left} + A_{right})}{2D} \tag{2.3}$$

The asymmetry of absorption band, *S*, of the feature represents the ratio of the area left (A_{left}) of absorption position to the area right (A_{right}) of absorption position as (Van der Meer, 1995, 2004):

$$S = \frac{A_{left}}{A_{right}} \tag{2.4}$$

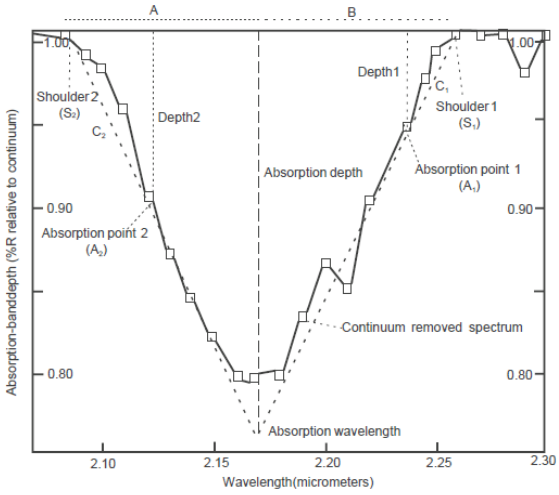

Figure 2.6. The absorption feature parameters of continuum removal spectrum used in the linear interpolation method (*Source:* Van der Meer, 2004: 59).

In a study of minerals mapping approach of hyperspectral remote sensing data using "a simple linear interpolation method", Van der Meer (2004, 2006b) stated that the simple linear method can be applied to map a specific mineral on the image based on the continuum removal absorption features of the mineral reflectance spectra through the following procedures and mathematical functions as depicted in Figure 2.6. In the first stage, user should determine the absorption feature of the image reflectance spectra for a specific mineral that would provide two appropriate shoulders, namely S_2 is a short wavelength shoulder and S_1 is a long wavelength shoulder. The process continues with continuum removal of the image at certain wavelength range indicating the mineral. Selecting two bands as absorption points (A_1 and A_2) for interpolation is the next stage. After this the coefficients C_1 and C_2 are computed using the formulas:

$$C_1 = \sqrt{(depth_1)^2 + (S_1 - A_1)^2} \qquad \text{and} \quad C_2 = \sqrt{(depth_2)^2 + (S_2 - A_2)^2} \tag{2.5}$$

The position of absorption wavelength, which is an interpolation result between the shoulders and absorption points in the spectrum, are given by

$$absorption\_wavelength = -\left[\frac{C_1}{C_1 + C_2} x\,(A_1 - A_2)\right] + A_1 \tag{2.6}$$

or

$$absorption\_wavelength = \left[\frac{C_2}{C_1 + C_2} x\,(A_1 - A_2)\right] + A_2 \tag{2.7}$$

The depth of absorption band can be derived from the following equations

$$absorption\_depth = \left[\frac{S_1 - absorption\_wavelength}{S_1 - A_1}\right] x\ depth_1 \tag{2.8}$$

or

$$absorption\_depth = \left[\frac{absorption\_wavelength - S_2}{A_2 - S_2}\right] x\ depth_2 \tag{2.9}$$

The asymmetry of absorption band is described by

$$asymmetry = A - B = (absorption\_wavelength - S_2) - (S_1 - absorption\_wavelength) \tag{2.10}$$

Where the result of calculation is 0 if the absorption feature is a perfect asymmetry, a negative value for a skewed absorption feature toward the shorter wavelength, and a positive value for a skewed absorption feature toward the longer wavelength.

3. Materials and Methods

3.1. Study Area

The study area is located in the Bédarieux mining area, which is an open and partly active dolomite mine with central coordinates are 43°37'N and 3°12'E, the Hérault department of Languedoc-Roussillon region, southeastern France (Figure 3.1). The outcrop based on the geological map is situated along the D908 which connects to Bédarieux Clermont l'Hérault, around 1 km from junction of Carlencas[1]. The dolomite mine is also surrounded by abandoned mines with some bauxite pockets inside the area. From a geological point of view, the area is a part of the consolidated rocks which is a transition zone between the coastal plain, the alluvial sediments of the Hérault River and the metamorphous rock of 'Massif Central' (Gèze, 1979). The area has unique geological structures ranging from sandstone formation, limestone plateaus, dolomite formation, and volcanic tuffs and volcanic basalt deposits (Sluiter, 2005).

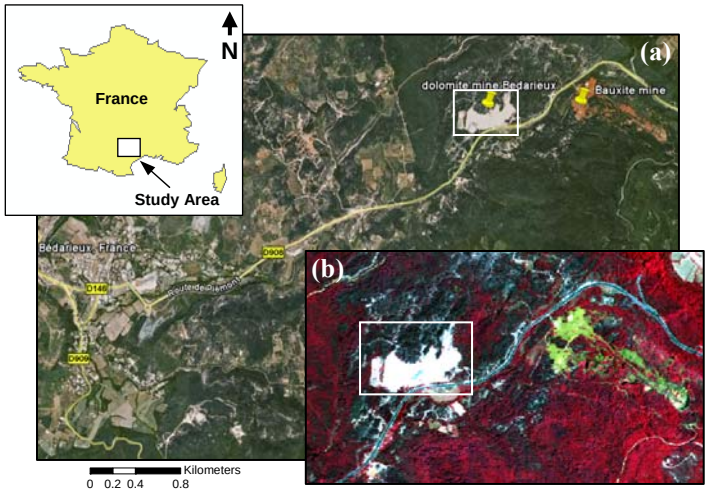

Figure 3.1. Location of the study area in the Bédarieux mining area, the Hérault department of Languedoc-Roussillon region, southeastern France *(Source: (a) Google maps, 2008; (b) HyMap2003 image).*

[1] http://pedagogie.ac-montpellier.fr/svt/litho/carlencas-dolomie/localisation.htm

3.2. Materials

The research that has been conducted needed several supporting materials such as data available, software, and instruments.

3.2.1. Data

- Minerals: calcite (pure powdered moura calcite marble) and dolomite (powdered chemical pure dolomite).
- Field or rock samples collected from the area between Bédarieux and Mourèze, southeastern France.
- Reflectance spectra of synthetic samples in the SWIR and TIR region and field samples in the SWIR band.
- The HyMap2003 image of the Bédarieux mining area, the Hérault department of Languedoc-Roussillon region, southeastern France.
- Geological Map of Bédarieux, scale 1 : 50,000 (1988)[1].

3.2.2. Software

- ENVI version 4.5 for spectral library building, resize of reflectance spectra, reflectance spectra analysis and the carbonate minerals mapping.
- DISPEC programme that are embedded within ENVI software for analysis of absorption features of reflectance spectra.
- ArcGIS version 9.3 for editing, compilation and visualisation results.
- Microsoft Excel for data processing and statistical analysis.

3.2.3. Instruments

- Bruker Vertex 70 FTIR Spectrometer for synthetic and field samples reflectance spectra acquisition in the SWIR and TIR region.
- Laboratory equipment for synthetic and field samples preparation and processing such as a set of laboratory jaw-crusher and steel percussion mortar and pestle, a set of laboratory sieve, furnace or oven, toploading precision balance (model: Mattler PE360), porcelain mortar and spoon-spatula, weight pressure, geological tools and sample containers.

3.3. Synthetic Sample Experiments

Synthetic sample experiments were performed strictly through a series of procedures and stages in the Geosciences Laboratory, ITC that involved sample preparations and reflectance spectra measurements. This research was conducted to analyse how

physical and chemical parameters such grain size fractions (Crowley, 1986; Gaffey, 1986; Salisbury *et al*., 1987; Van der Meer, 1994; 1995; Clark, 1999), packing or porosity (Gaffey, 1986), and mineral contents or mineral mixtures (Gaffey, 1985; Salisbury *et al*., 1987; Van der Meer, 1994; 1995; Clark, 1999) affecting the spectral characteristics of the carbonate synthetic samples. The objective of the research are to characterize the absorption features of the pure powdered moura calcite marble and chemical pure dolomite reflectance spectra in the SWIR and TIR region based on the synthetic samples in order to identify changes of spectral characteristic as a function of grain size fractions, packing models, and mineral contents.

3.3.1. Sample Preparations

3.3.1.1. Synthetic Sample of Pure Powdered Calcite and Dolomite

Rock samples of moura calcite marble and chemical pure dolomite (Figure 3.2), which were provided by the Geosciences Laboratory, were pulverised separately into a powder by a laboratory jaw-crusher and a steel percussion mortar and pestle. After that the samples were put into separate container and dried in an oven or furnace at 105^{o}C over a night to evaporate water molecule inside the powdered minerals. The pulverised moura calcite marble and chemical pure dolomite were then sieved into six different grain size fractions which varied from fine to coarse with a diameter between 45 μm and 500 μm by a set of laboratory sieve as illustrated in Table 3.1.

Figure 3.2. Rock samples of moura calcite marble and chemical pure dolomite before crushed.

The process was continued with packing of the samples, where the powdered minerals of moura calcite marble and chemical pure dolomite were placed into an aluminium case or container with a diameter 5 cm and thick 5 mm and pressed using weight or load pressure on the top of the samples for 5 minutes. Three types of packing models have been set up for each synthetic sample from loose to compact packing samples (Figure 3.3) as followed:

(a) loosely stacked packing sample (without pressure; model 0)
(b) compact packing sample with weight pressure 1090 grams (model 1)
(c) compact packing sample with weight pressure 2200 grams (model 2)

Table 3.1. The diameter of grain size fractions of the pure powdered moura calcite marble and chemical pure dolomite.

No.	Grain Size Fractions (µm)
1.	Less than 45
2.	45 – 90
3.	90 – 125
4.	125 – 250
5.	250 – 500
6.	Greater than 500

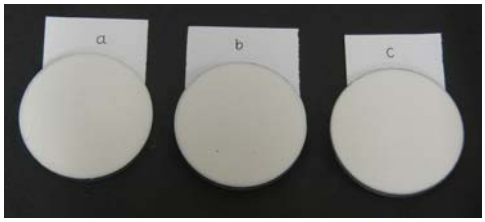

Figure 3.3. The differences in packing models of the pure powdered moura calcite marble with grain size fractions 125 - 250 µm.

All the procedures were strictly controlled to avoid any possible contamination of the samples. Finally the reflectance spectra of the synthetic samples were ready measured using the Bruker Vertex 70 FTIR Spectrometer.

3.3.1.2. Synthetic Sample of Powdered Calcite and Dolomite Mixtures

The mixing between the calcite and dolomite, based on the differences in mineral contents and grain size fractions, has been conducted through the sequence of laboratory experiments in Geosciences Laboratory, ITC. The synthetic samples of the moura calcite marble-chemical pure dolomite mixtures used in these experiments consisted of three different grain size fractions such as less than 45, 45-125, and 125-500 µm instead of using six different grain size fractions as mentioned in previous section of the minerals. It was performed because the quantity of the minerals for each grain size fractions were shortage to design a number of various synthetic samples with different mineral contents and grain size fractions. These synthetic samples that have been prepared however could still represent the fine and the coarse grain size fractions of the minerals.

In terms of sample preparations of the calcite and dolomite mixtures with different mineral contents and the same grain size fractions, in the first stage an empty plastic

box as sample container was weighed to keep a steady total amount of the mixing minerals. Then the pure powdered moura calcite marble and powdered chemical pure dolomite were put into the plastic container and weighed on the basis of weight percentage of each mineral in the total weight of the sample respectively, using a top-loading precision balance (model: Mattler PE360) with a reading precision ± 1 mg. The total amount of the minerals needed to prepare a synthetic sample were approximately 25 grams and the compositions of the calcite-dolomite mixtures with different mineral contents are provided in the Appendix II.

The stirring process was the next stage in order to obtain a homogenous synthetic sample of the calcite-dolomite mixtures. The calcite and dolomite that have been weighed were fed into a porcelain mortar and stirred manually using a spoon-spatula for 10 minutes. After that the homogenous mixing minerals were placed into an aluminium case with a diameter 5 cm and thick 5 mm and pressed based on compact packing sample (model 1) for 5 minutes. Furthermore, the synthetic samples of the mixing between the pure powdered moura calcite marble and chemical pure dolomite with different grain size fractions and the same weight percentage of each mineral were also prepared with the same procedures as mentioned above. The detail compositions of the calcite-dolomite mixtures with different grain size fractions can be seen in the Appendix II. All the procedures were strictly controlled to avoid any possible contamination of the samples. Finally the reflectance spectra of the synthetic samples were ready measured by the spectrometer.

3.3.2. Reflectance Spectra Measurements

Fourier Transform Infrared (FTIR) spectroscopy has been widely used for analysis of organic and inorganic matters (Bertaux *et al.*, 1998; Reig *et al.*, 2002), because it only needs a few amounts of sample, fast and simple sample preparation, and less time consuming for analysis (Reig *et al.*, 2002). In addition, the equipment that is usually used for recording spectra of the matters is FTIR spectrometer. The spectrometer is controlled by an interferometer as the core component. This instrument splits and recombines a beam of light such as the IR source which produces a wavelength-dependent interference pattern or an interferogram. The interferogram containing the essential information on the basis of frequencies and intensities of the matters should be converted using Fourier Transform methods in order to obtain a real spectrum (Griffiths and De Haseth, 2007).

This research used the Bruker Vertex 70 FTIR Spectrometer for measuring reflectance spectra of the pure and mixing of powdered moura calcite marble and chemical pure dolomite in the SWIR region between 1.0 μm and 3.3 μm. Before

measuring reflectance spectra of the minerals in the SWIR band, the NIR beam splitter must be put in the appropriate place of the spectrometer and the NIR lamp should be warmed up approximately 45 minutes. The procedures must be activated through the OPUS software within the computer system which has been integrated with the spectrometer, particularly the NIR source and detector. After that the carbonate mineral samples were placed on the top of laboratory jack and raised as close as possible to the sample port of spectrometer. So that the optical path of the radiation emitted by the source to the sample and reflected by the sample to the detector become shorter and in the form of maximum intensity, and the radiation reflected by the sample can reach the detector properly.

The process was continued with several parameters setting of the spectrometer in the SWIR using the OPUS software as followed. These parameters that have been set by mean of the OPUS software can be explored in more detail in the Appendix III.

Resolution	: 16 cm^{-1} (wave number)
Sample scan time	: 256 scans
Background scan time	: 256 scans
Save data from	: 10,000 cm^{-1} to 3000 cm^{-1}
Result Spectrum	: Reflectance

For measuring reflectance spectra of the samples, each sample was scanned twice on the same surface by the spectrometer respectively. In the first step, the spectrometer scanned the sample as background or reference single channel (RSC) by switching the mode to the reference channel and wait until the measurement completed. The mode was then switched to the sample channel in order to scan the sample as sample single channel (SSC). Reflectance spectra resulted by the spectrometer are the ratio of SSC to RSC in measuring of the sample at a sequence time. Moreover, the software can also be used to convert the spectra of the minerals acquired by the spectrometer from wave number to wavelength and save it into ASCII format or data point table (dpt) for building a spectral library of the minerals in the ENVI.

The thermal infrared reflectance spectra of the pure and mixing of the powdered calcite and dolomite were also measured by the Bruker Vertex 70 FTIR Spectrometer in the wavelength range of 1.0 - 20 μm. Basically, the procedures used for measuring reflectance spectra of the sample in the TIR were same as the SWIR method as mentioned above, but several parameters must be adjusted. Firstly, the NIR beam splitter must be changed with the MIR (mid-infrared) beam splitter. Water cooling in order to cool the external TIR source must be then turned on a few minutes before turned on power supply of the external TIR source. After this the

TIR detector must be cooled by liquid nitrogen and the spectrometer should be warmed up approximately 45 minutes before acquisition of the reflectance spectra. In the final stage, a number of the spectrometer parameters were set using the OPUS software and these parameters are available in more detail in the Appendix III.

Resolution	: 8 cm^{-1} (wave number)
Sample scan time	: 4096 scans
Background scan time	: 4096 scans
Save data from	: 10000 cm^{-1} to 500 cm^{-1}
Result Spectrum	: Reflectance

3.4. Field Sample Experiments

Field sample experiments have been conducted in subsequent procedures and stages in the study area and the Geosciences Laboratory, ITC that involved field sample collection, sample preparations, and reflectance spectra measurements. This research was performed to analyse the kind of carbonate minerals available in the field samples. The objective of the research are to identify the diagnostic absorption features in the SWIR of the carbonate rock samples collected from the area between Bédarieux and Mourèze, southeastern France.

3.4.1. Field Sample Collection

Field samples or rock samples were collected from several locations in the area between Bédarieux and Mourèze, the Hérault department of Languedoc-Roussillon region, southeastern France during a fieldwork in September 2008 by the Utrecht University research team. The rock samples were selected from specific locations in the study area consisting of the north of the Bédarieux mining area (sample 11, 12, and 36) which is an abandoned mine with some bauxite pockets in this area, the dolomite mine in the Bédarieux mining area (samples 14 to 29), the dolomite mine in the Mourèze area (samples 30 to 35), and a number of rocks in other sites within the area such as sample 13 collected form southwestern of the Bédarieux mine, sample 37 which is a bauxite sample collected in the bauxite mine, the southeastern of Levas, Carlencas, and sample 38 which is a limestone sample collected from the northwestern of Lodève, far to the north outside of the HyMap lines. The total rock samples collected from the area, based on the information on the geological maps and the HyMap2003 image, were 28 samples and the sample positions in the selected locations were determined by a hand-held GPS in XY-direction with the coordinate system in UTM WGS84 zone 31 N. The detail descriptions of the field samples collection carried out in the study area are provided in the Appendix IV.

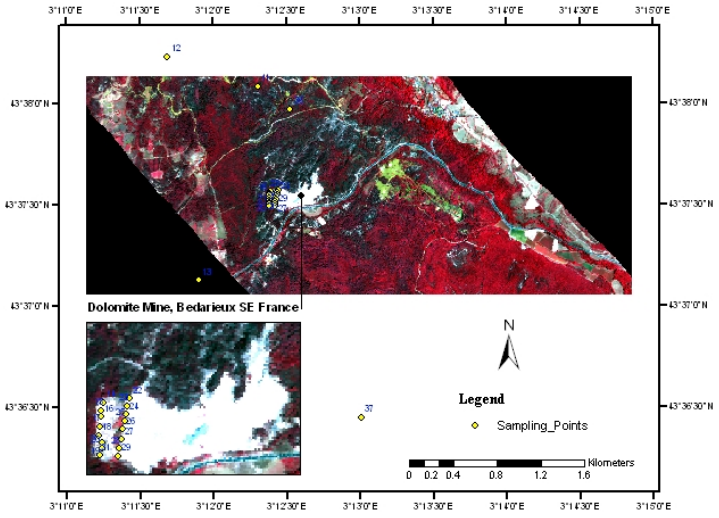

Figure 3.4. A standard colour infrared of the HyMap2003 image and sampling point locations in the Bédarieux mining area, southeastern France.

The majority of rock samples were positioned within the HyMap2003 image as shown in Figure 3.4, but there were also several samples which were located in the outside of the HyMap data, especially a transect of the rock sample from the dolomite mine in the Mourèze area. Nevertheless, the samples are quite useful to identify more variability of the dolomite or carbonate rocks occurrences between Bédarieux transect and Mourèze transect. In addition, every rock sample collected in the selected locations was accompanied by a field picture and some remarks related to the occurrence of its conditions in the fields. The focus of collection field data, particularly for validation purpose between the classified HyMap data and ground truth data was in the Bédarieux mining area which is an open and partly active dolomite mine and assigned as white colour of a standard colour infrared of the HyMap2003 image in the western part of the region (Figure 3.4). Two transects of the rock samples were collected in the study area which consisted of samples 14 to 21 in the western transect of the dolomite mine and samples 22 to 29 in the eastern transect of the mine. These samples were then delivered to the Geosciences Laboratory, ITC for preparing, measuring, and analysing reflectance spectra.

3.4.2. Field Sample Preparations

In the first instance, the rock samples were prepared in order to obtain a fresh and flat rock surface as much as possible with a diameter at least 3 cm for matching with the sample port of the spectrometer by a set of laboratory equipment in the

Geosciences Laboratory. The preparation must be done correctly and patiently because a number of the rocks seemed like a sandy carbonate rock that can break easily. The fresh surfaces of the rock samples are essential to avoid the natural impurity layer of the rocks, for instance organic matters hinder the true reflectance of the rock materials so that the reflectance spectra recorded from not fresh rock surface are not real spectral features of the minerals forming the rock.

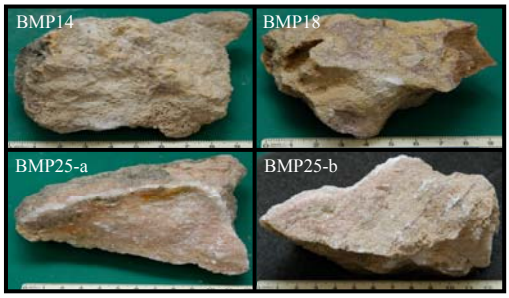

Figure 3.5. The fresh surfaces of the rock samples collected from Bédarieux transect.

Furthermore, the flat rock surfaces are needed because the rocks can be fed as close as possible to the electromagnetic source and detector of the SWIR through the spectrometer acquisition. The process was continued with capturing a picture of the fresh rock surfaces for reference and highlight the surface that will be measured its reflectance spectra using the Bruker Vertex 70 FTIR Spectrometer in the SWIR region.

3.4.3. Reflectance Spectra Measurements

Reflectance spectra of the rock samples in the SWIR band were measured using the Bruker Vertex 70 FTIR Spectrometer. The reflectance spectra of the field samples were only recorded in the SWIR region, because the carbonate absorption features can be identified in the SWIR band and the HyMap2003 data, which were used for mapping the carbonate minerals and validation the classified image with the laboratory spectra of the rocks, only have the spectral range in the 0.45-2.5 μm from the visible to SWIR. The spectrometer parameters and procedures that have been used for acquisition the reflectance spectra of the field samples were exactly same as the previous setting for measuring the synthetic samples in the SWIR band.

3.5. Reflectance Spectra Analysis

The reflectance spectra of the synthetic and field samples in the SWIR region, especially absorption features of the spectra were analysed using the DISPEC

programme that are embedded within the ENVI software and the tools are exactly located inside the spectral menu. The spectra that would be analysed by the programme were only the strongest absorption features of the reflectance spectra. The spectra were then cut into specific reflectance spectra of the pure calcite and dolomite in the wavelength range of 2.164-2.653 μm indicating the strongest vibrational absorption features. When the subset processes are performed through the ENVI, the carbonate minerals spectra should be cut at the proper wavelength band of its diagnostic absorption features from the left (shorter wavelength) to the right side (longer wavelength) of the features in order to obtain appropriate shoulders. So that the absorption features of the spectra could be computed correctly by the programme.

The subset spectra were then selected as input file of the DISPEC programme. Before analysing the absorption features of the spectra, several parameters must be adjusted by mean of the DISPEC TOO window such as *absolute shoulder* as *End of feature* and *additive* as *Hull application*.

The absorption features calculated by the programme based on the continuum removal spectra consisted of position or centre of absorption band (λ), depth of absorption band (D), width of absorption band (*Width*), and asymmetry of absorption band (S). The formulas used for computing the absorption features are precisely same as the formulas that have been stated in the literature review (Equation (2.2), (2.3) and (2.4)).

Moreover, the absorption features of the pure and mixing of the powdered moura calcite marble and chemical pure dolomite reflectance spectra in the TIR band were also analysed using the DISPEC programme. The spectra that were investigated by the programme were cut into the diagnostic reflectance spectra or the strongest vibrational absorption features of the pure calcite and dolomite in the TIR with wavelength range between 10.0071μm and 15.0054μm. In general, the absorption features were calculated using the same DISPEC parameters and procedures as mentioned previously, but these parameters did not work perfectly for the coarse grain size fractions, particularly on the second absorption feature of the pure and mixture of synthetic samples due to higher absorption of the thermal energy by the coarse grain size fractions of the minerals. Consequently the programme could not find the proper shoulders on the left and the right side of the feature. In this case, the second feature of spectral reflectance of the synthetic samples can be analysed by the programme, if the *Hull application* parameter was changed from *additive* to *multiplicative* and *maximum value* was used as the *End of feature* but the absorption

features resulted altered considerably. Therefore, it was relatively difficult to interpret the absorption features of the reflectance spectra of the carbonate mineral in the TIR region.

3.6. Hyperspectral Image Processing and Mapping Method

The HyMap2003 airborne hyperspecral imagery was processed through several subsequent steps using the ENVI software. In the first instance, vegetations covering the study area on the image were masked using a Normalized Difference Vegetation Index (NDVI) with the input data range for masking was 0.6. After this the absorption features of the carbonate minerals were identified. Subset and continuum removed image at certain wavelengths that indicate the diagnostic absorption features of the minerals in the range of 2.1710-2.4050 µm or from band 107 to 121 of the HyMap data were the next step. It was conducted because the strong absorption features of the carbonate minerals in the image were at these bands.

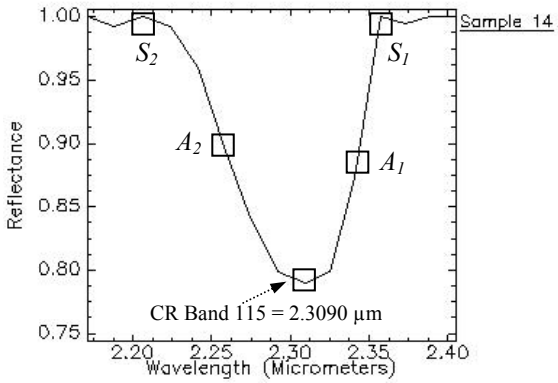

Figure 3.6. The continuum removal spectrum of carbonate absorption band with wavelength range between 2.1710 µm and 2.4050 µm derived from the location of the sample 14 in the HyMap2003 image.

In terms of calcite and dolomite mapping for assessing dolomitization patterns in the study area, "a simple linear interpolation method" based on the work of Van der Meer (2004, 2006b) was applied to the HyMap image with a series of spectral features processing. The approach as stated in the literature review (Van der Meer, 2004; 2006b) uses the continuum removal (CR) absorption features of the minerals' reflectance spectra through the following procedures and mathematical functions. First, the continuum removed absorption features of the carbonate minerals from the HyMap data that would provide two appropriate shoulders were determined as depicted in Figure 3.6. Where S_1 is a long wavelength shoulder and S_2 is a short

wavelength shoulder. The process continued with selecting two bands as absorption points (A_1 and A_2) for interpolation. After this the coefficients C_1 and C_2, absorption wavelength, absorption depth, and asymmetry were computed using the following scripts based on the equation (2.5) to (2.10) in the band math operator of the ENVI software. From the graph is obvious that shoulders (S_1 and S_2) and absorption points (A_1 and A_2) can be determined for calculating the coefficients C_1 and C_2:

S_1 = CR band 118 (2.3570 µm); S_2 = CR band 109 (2.2060 µm)
A_1 = CR band 117 (2.3410 µm); A_2 = CR band 112 (2.2580 µm)

The coefficients C_1 and C_2 were computed using the following scripts:

C_1 = float (sqrt(((1-b1)^2)+((2.3570-2.3410)^2)))
Where, b1 = CR band 117 (2.3410 µm)

C_2 = float (sqrt(((1-b1)^2)+((2.2060-2.2580)^2)))
Where, b1 = CR band 112 (2.2580 µm)

The position of absorption wavelength was computed using the scripts:

Absorption wavelength 1 = float (2.3410-((b1/(b1+b2))(2.3410-2.2580)))*
Where, b1 = C_1; b2 = C_2; *or*

Absorption wavelength 2 = float (2.2580+((b1/(b1+b2))(2.3410-2.2580)))*
Where, b1 = C_2; b2 = C_1

The depth of absorption band can be derived from the following script:

Absorption band depth = float (((2.3570-b1)/(2.3570-2.3410))(1-b2))*
Where, b1 = *Absorption wavelength 1*; b2 = CR band 117 (2.3410 µm)

The asymmetry of absorption band is given by the script:

Asymmetry = float ((b1-2.2060)-(2.3570-b1))
Where, b1 = *Absorption wavelength 1*

Finally, the results of this approach, which indicated the absorption features of the carbonate minerals and dolomitization patterns in the study area, were validated using the ground truth data or laboratory spectra of the field samples. The validation process only compared the laboratory spectra of the synthetic samples with field samples and fields samples collected from the two transects of the Bédarieux's dolomite mine with the HyMap spectra derived from the same locations.

4. Results

This chapter describes the results of reflectance spectra and absorption features of the synthetic sample and field or rock samples and calcite-dolmite mapping of the HyMap data using simple linear interpolation method. The diagnostic absorption features of the synthetic samples reflectance spectra, which are the pure and mixing of powdered moura calcite marble and chemical pure dolomite, as a function of grain size fractions, packing models, and mineral contents in the SWIR and TIR are presented in the first section. The second section explains the SWIR absorption features of the rock samples reflectance spectra collected from the area between Bédarieux and Mourèze in order to identify types of carbonate minerals forming the rock. These spectral features of the synthetic and rock samples can be used as a preliminary proxy for assessing dolomitization patterns in the study area. The third section describes diagnostic absorption features of carbonate minerals derived from the HyMap data and calcite-dolomite mapping results for assessing dolomitization patterns using simple linear interpolation method. The last section presents validation results of the absorption features of the carbonate minerals and dolomitization patterns in the study area using the HyMap data and the ground truth data or laboratory spectra of the field samples.

4.1. Absorption Features of Synthetic Samples in the SWIR and TIR

Reflectance spectra in the SWIR and TIR contain a number of absorption features which can be used for discrimination between carbonate minerals and other minerals and identification of calcite and dolomite with another carbonate mineral. This section presents results of various physical and chemical parameters influencing the absorption features of reflectance spectra of the pure and mixture of calcite and dolomite in the SWIR and TIR. The results are divided into several meaningful sections such the absorption features of the synthetic samples of the pure powdered moura calcite marble and chemical pure dolomite with different grain size fractions and packing models in the SWIR; the absorption features of the pure synthetic samples with different grain size fractions in the TIR; the absorption features of the synthetic samples of the powdered moura calcite marble and chemical pure dolomite mixtures with different mineral contains and grain size fractions in the SWIR; and the absorption features of the mixture synthetic samples with different mineral contains and grain size fractions in the TIR.

4.1.1. Absorption Features of the Pure Calcite and Dolomite with Different Grain Size Fractions and Packing Models in the SWIR

The results of the absorption features analysis of the pure powdered moura calcite marble and chemical pure dolomite reflectance spectra with different grain size fractions in the SWIR are reported. The grain size fractions of the minerals used in this study are from fine to coarse grain size with the diameter between 45 μm and 500 μm as provided in Table 3.1. Figure 4.1 shows the reflectance spectra of the pure powdered moura calcite marble and chemical pure dolomite with different grain size fractions and the same packing model with weight pressure 1090 grams (model 1) in the range of 1.0011-2.6526 μm and 2.164-2.653 μm. These diagnostic spectra visually illustrate that the strongest vibrational absorption features for the calcite occur around 2.34 μm and 2.54 μm and the strongest vibrational absorption features for the dolomite occur around 2.32 μm and 2.51 μm. The occurrence of the carbonate minerals can also be recognized from the weak absorption features that occurred at 1.86, 1.98, and 2.14 μm for the dolomite and at 1.87, 1.99, and 2.15 for the calcite. It indicates that both of the carbonate minerals composing the synthetic samples are pure calcite and dolomite.

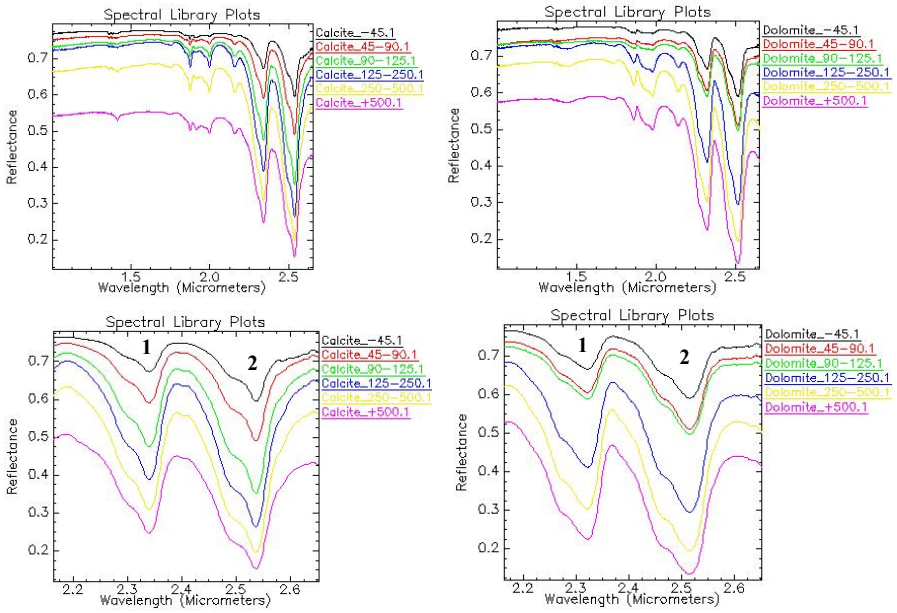

Figure 4.1. Reflectance spectra of the pure powdered moura calcite marble and chemical pure dolomite with different grain size fractions and the same packing model (model 1) in the range between 1.0011 μm and 2.6526 μm and 2.164 μm and 2.653 μm.

It is also obvious from the graphs that the differences in grain size fractions of the calcite and dolomite influence its spectral features, especially depth of absorption band and overall brightness of the minerals in the SWIR. The depth of absorption band increase considerably with increasing grain size fractions of calcite and dolomite, whereas the overall brightness of the minerals decrease significantly with increasing grain size fractions. The exact absorption features consisting position of absorption band, depth of absorption band, width of absorption band, and asymmetry of absorption band of the calcite and dolomite are calculated using the DISPEC programme embedded within the ENVI software. The features only consider to the strongest vibrational absorption features of the calcite and dolomite in the SWIR spectra (2.164 - 2.653 μm) as depicted in Figure 4.1.

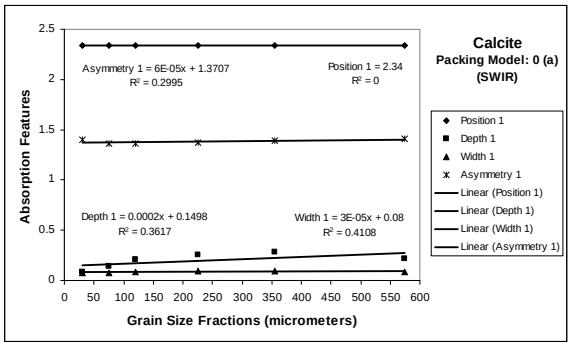

(a)

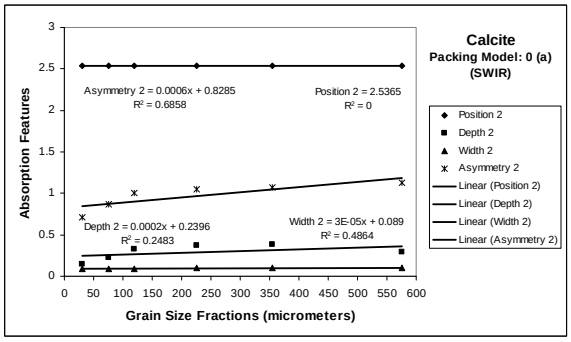

(b)

Figure 4.2. Absorption features of the pure powdered moura calcite marble reflectance spectra at 2.34 μm and 2.5365 μm as a function of grain size fractions for the same packing model (model 0).

Figure 4.2 indicates the position, depth, width, and asymmetry of absorption band of reflectance spectra of the calcite as a function of grain size fractions for the same

packing models in the SWIR. The graphs describe that only the positions of absorption band for both features (the first and second feature) are invariant with grain size fractions. It is clear from the graph that the pure powdered moura calcite marble has two characteristic positions of absorption band in the SWIR centred at 2.34 μm for the first feature (Figure 4.2 (a)) and 2.5365 μm for the second feature (Figure 4.2 (b)). The positions of the calcite absorption wavelength in the SWIR, which are caused by vibrational absorption of carbonate ion (CO_3^{-2}), are located at a slight micrometers higher wavelength than the dolomite.

Conversely, these absorption features indicate that depths of absorption band of the reflectance spectra increase considerably with increasing grain size fractions. It reveals that coarse grain size fractions of the mineral are deeper absorption features than the fine grain size fractions due to brightness factors (Gaffey, 1986; Van der Meer, 1994; 1995) and internal optical path (Clark and Roush, 1984). The fine grain size fractions of the mineral are brighter and shorter internal optical path than the coarse grain size fractions so it absorbs less electromagnetic radiation that penetrate to the surface of the minerals. The width and asymmetry of absorption band vary slightly with grain size fractions. The widths and asymmetries of absorption band of the calcite increase slightly with increasing grain size fractions. It shows that the asymmetries of the absorption features are strongly skewed to longer wavelength. The absorption features of the calcite as a function of grain size fractions for other packing models are provided in the Appendix V.

Figure 4.3 illustrates the position, depth, width, and asymmetry of absorption band of reflectance spectra of the dolomite as a function of grain size fractions for the same packing models in the SWIR. The graphs describe that the position, width, and asymmetry of absorption band for both features vary with grain size fractions. It can be seen from the graph that the positions of absorption wavelength of the mineral are nearly invariant with grain size fractions. The first feature (Figure 4.3 (a)) of powdered chemical pure dolomite has diagnostic positions of absorption wavelength in the SWIR centred at 2.32293 μm for grain size fractions in the range of 45-125 μm and 2.32138 μm for grain size fractions in the range of 125-500 μm. The second feature (Figure 4.3 (b)) of powdered chemical pure dolomite has diagnostic positions of absorption wavelength in the SWIR centred at 2.51485 μm for grain size fractions in the range of 45-125 μm and 2.5133 μm for grain size fractions in the range of 125-500 μm. The positions of absorption band of the dolomite with the grain size fractions between 45 and 125 μm in the both features shift slightly to the longer wavelength. While the positions of absorption band of the dolomite with the grain size fractions between 125 and 500 μm in the both features shift slightly to the

shorter wavelength. It may be caused by the amount of Mg in the sample as stated by Gaffey (1985) that chemical composition will influence position of absorption band. The coarse grain size fractions are probably content more Mg than the fine grain size fractions.

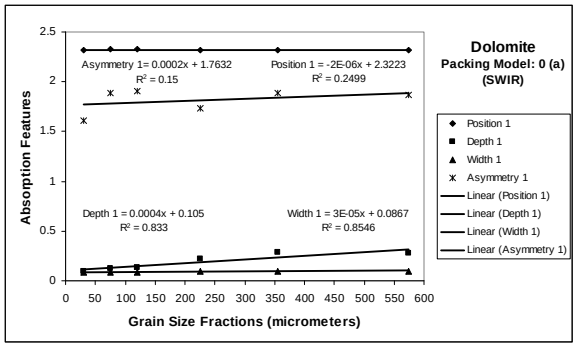

(a)

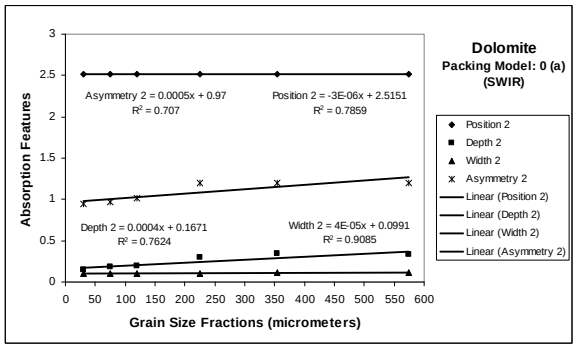

(b)

Figure 4.3. Absorption features of the chemical pure dolomite reflectance spectra at 2.32 μm and 2.51 μm as a function of grain size fractions for the same packing model (model 0).

These absorption features also illustrate that the depths of absorption band of spectral reflectance vary substantially with grain size fractions. There is a significant increase in depths of absorption band when grain size fractions increase from the fine to the coarse grain size. It is obvious from the graph that the coarse grain size fractions are deeper absorption features than the fine grain size fractions due to brightness factors and internal optical path. As mentioned previously that the fine grain size fractions are brighter and shorter optical path than the coarse grain size fractions of powdered chemical pure dolomite. The graph also shows that the

asymmetries of the absorption features increase slightly with increasing grain size fraction of the mineral. It indicates that the asymmetries of absorption features of the dolomite are strongly skewed to longer wavelength. The absorption features of reflectance spectra of the powdered chemical pure dolomite as a function of grain size fractions for other packing models are provided in the Appendix V. Consequently, the difference in grain size fractions only influence significantly the depths of absorption bands of reflectance spectra of the pure powdered moura calcite marble and chemical pure dolomite in the SWIR, although the sample packing models of the minerals are varied from loose to compact packing sample.

4.1.2. Absorption Features of the Pure Calcite and Dolomite with Different Packing Models in the SWIR

The results of the absorption features analysis of the moura calcite marble and chemical pure dolomite for each grain size fractions with different packing models or porosity in the SWIR are presented. The sample packing models of the minerals used in this research are from loose to compact packing models. The packing models consist of loosely stacked packing sample (model 0), compact packing sample with weight pressure 1090 grams (model 1), and compact packing sample with weight pressure 2200 grams (model 2). Figure 4.4 reveals the position, depth, width, and asymmetry of absorption band of reflectance spectra of the calcite as a function of three different types of packing models for each grain size fractions in the SWIR. The graphs describe that the positions of absorption wavelength for both features (the first and second feature) are invariant with the sample's packing models as well as the widths of absorption band are nearly invariant with the packing models. It is clear from the graph that the pure powdered moura calcite marble has two diagnostic positions of absorption wavelength in the SWIR centred at 2.34 μm for the first feature (Figure 4.4 (a)) and 2.5365 μm for the second feature (Figure 4.4 (b)). These absorption wavelength positions of the calcite in the SWIR are caused by vibrational absorption processes of carbonate ion (CO_3^{-2}).

However, the graphs also illustrate that the depth and asymmetry of absorption band vary slightly with the aspect of sample packing models. In general, loosely stacked packing samples are marginally deeper spectral absorption than compact packing samples or the depths of absorption band decrease slightly with increasing the compact of packing models as stated by Gaffey (1986). It may be caused by the smoothness or texture of the sample surface. The loosely stacked packing sample seems rougher surface than compact packing sample so it absorbs more electromagnetic radiation. Whereas the asymmetries of absorption band increase

slightly with increasing the compact of packing models and it indicates that the asymmetries of absorption features are strongly skewed to longer wavelength.

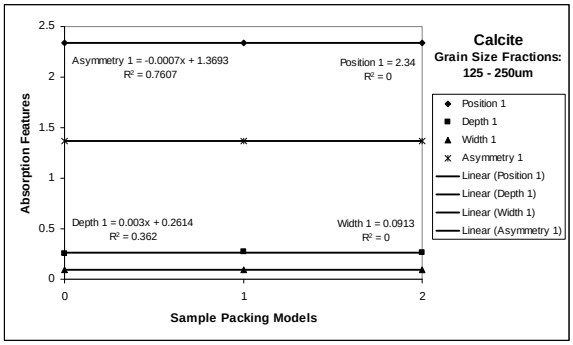

(a)

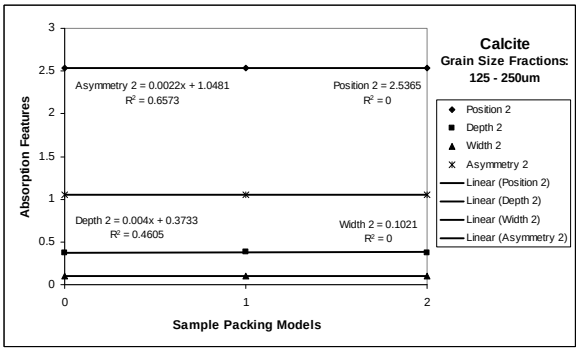

(b)

Figure 4.4. Absorption features of the pure powdered moura calcite marble reflectance spectra at 2.34 μm and 2.5365 μm as a function of packing models with grain size fractions 125-250 μm.

Figure 4.5 represents the position, depth, width, and asymmetry of absorption band of reflectance spectra of the dolomite as a function of three different types of packing models for each grain size fractions in the SWIR. The graphs illustrate that the positions of absorption band for both features are nearly invariant with sample packing models as well as the widths of absorption band. It can be seen from the graph that the powdered chemical pure dolomite has two diagnostic positions of absorption wavelength in the SWIR centred at 2.32 μm for the first feature (Figure 4.5 (a)) and 2.51 μm for the second feature (Figure 4.5 (b)). The position of the dolomite absorption wavelength is located at a slight micrometers lower wavelength than the calcite.

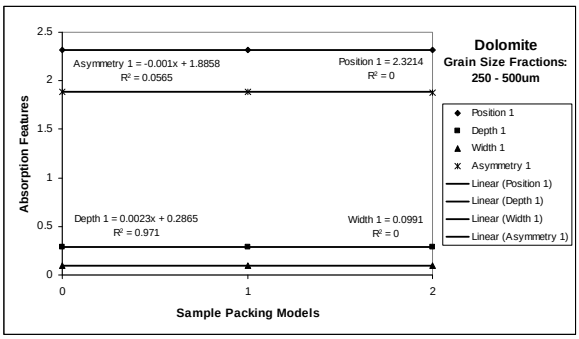

(a)

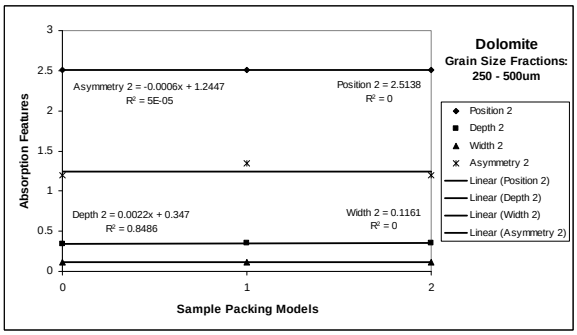

(b)

Figure 4.5. Absorption features of the chemical pure dolomite reflectance spectra at 2.3214 μm and 2.5138 μm as a function of packing models with grain size fractions 250-500 μm.

Nevertheless, the graphs also indicate that the depth and asymmetry of absorption band vary slightly with aspect of sample packing models. In general, loosely stacked packing samples are marginally less reflectance value than compact packing samples or the depths of absorption band decrease slightly with increasing the compact of packing models, whereas the asymmetries of absorption band increase slightly with increasing the compact of packing models. It indicates that the asymmetries of absorption features are strongly skewed to longer wavelength. As a result, the differences in the sample packing models does not influence significantly the absorption features of reflectance spectra of the pure powdered moura calcite marble and chemical pure dolomite, although the grain size fractions of the minerals vary from fine to coarse grain size fractions. So that for further spectral measurements of the pure synthetic samples in the TIR and the mixture synthetic samples in the SWIR and TIR only use the compact of packing model one.

4.1.3. Absorption Features of the Pure Calcite and Dolomite with Different Grain Size Fractions in the TIR

The results of the absorption features analysis of the calcite and dolomite spectra with different grain size fractions in the TIR are described. This study used the same grain size fractions of the minerals as the previous experiment in the SWIR. While the sample packing model used is the compact of packing model one. Figure 4.6 represents the absorption features of reflectance spectra of the calcite and dolomite with different grain size fractions and the same packing model (model 1) in the range of 10.8900-14.8083 µm. These diagnostic spectra visually illustrate that the strongest vibrational absorption features for both of the minerals are shifted substantially by increasing the grain size fractions of the minerals in the TIR region. The absorption band positions of the first feature of the minerals shift to longer wavelength while the second feature shift to shorter wavelength. In the same way, the depth, width, and asymmetry of absorption features vary when grain size fractions change from fine to coarse, whereas the brightness of the spectra decreases significantly when the diameter of grain size fractions increases.

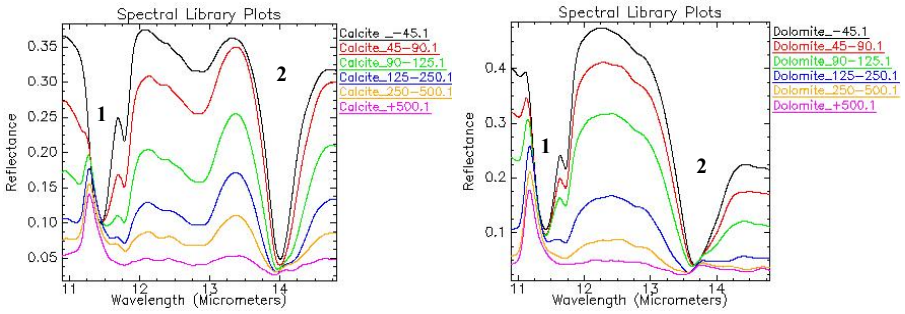

Figure 4.6. Reflectance spectra of the pure powdered moura calcite marble and the powdered chemical pure dolomite with different grain size fractions and the same packing model (model 1) in the range of 10.8900-14.8083 µm.

The positions of absorption band of the reflectance spectra of the pure powdered moura calcite marble as a function of grain size fractions for the same packing models in the TIR are shown in Figure 4.7. There are significant shifts in the positions of absorption band for both of the features when grain size fractions of the mineral increase. The characteristic positions of absorption band of the calcite in the TIR are at roughly in the range of 11.45 – 11.75 µm for the first feature and 14.00 – 13.92 µm for the second feature. In addition, Figure 4.8 illustrates the positions of absorption band of the reflectance spectra of the chemical pure dolomite as a

function of grain size fractions for the same packing models in the TIR. The graph indicates that the positions of absorption band also vary substantially with the grain size fractions. The diagnostic positions of absorption band of the dolomite in the TIR are at roughly in the range of 11.42 – 11.67 μm for the first feature and 13.65 – 13.44 μm for the second feature. It is clear from the graphs that the absorption band positions of these minerals in the TIR are dependent on the grain size fractions. The shifting of absorption band positions may be caused by the bending vibrational absorption of the carbonate ion (CO_3^{-2}) as stated by Salisbury *et al*. (1987). The position of the calcite absorption wavelength is located at a slight micrometers higher wavelength than the dolomite.

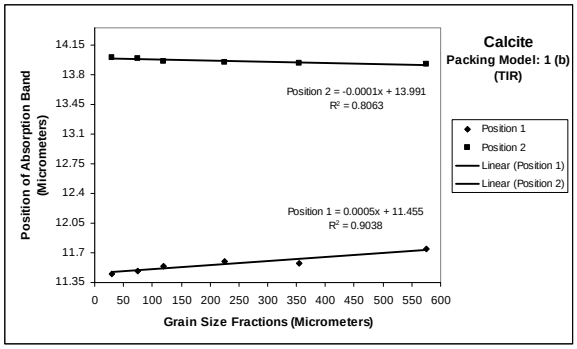

Figure 4.7. Positions of absorption band of the pure powdered moura calcite marble in the range of 11.45 – 11.75 μm and 14.00 – 13.92 μm as a function of grain size fractions.

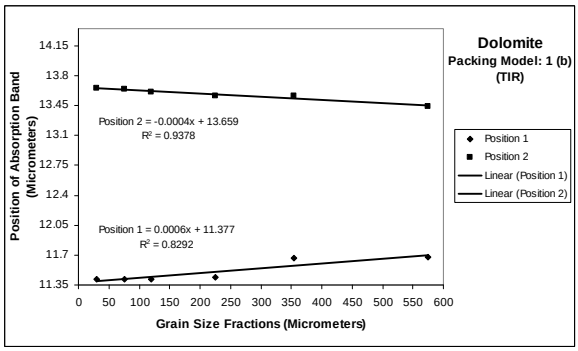

Figure 4.8. Positions of absorption band of the powdered chemical pure dolomite in the range of 11.42–11.67 μm and 13.65–13.44 μm as a function of grain size fractions.

Furthermore, the depth, width, and asymmetry of both absorption features of the calcite and dolomite in the TIR also vary with the grain size fractions as illustrated by the graph in the Appendix VI. However, these absorption feature parameters are relatively difficult to analyse, because the DISPEC programme did not work perfectly for calculating reflectance spectra of the coarse samples due to higher absorption of the thermal energy by the minerals. So it affects the absorption feature shape of the coarse sample, especially shoulders of the features almost disappear (Figure 4.6).

Generally, the depth of absorption band for the first and second feature decreases substantially when grain size fractions changes from fine to coarse, while the width of absorption band increase with increasing grain size fractions. The coarse grain size fractions absorb almost all of electromagnetic radiation that penetrates to the grain surface due to brightness factors and internal optical path. The brightness of the spectra decreases considerably when the diameters of grain size fractions increase. Moreover, the asymmetry of the first absorption feature is weakly skewed to longer wavelength, whereas the asymmetry of the second absorption feature is weakly skewed to shorter wavelength. As a result, the shape of spectral features and the absorption features of the pure powdered moura calcite marble and chemical pure dolomite in the TIR are influenced considerably by the grain size fractions.

4.1.4. Absorption Features of the Calcite and Dolomite Mixtures with Different Mineral Contents and Grain Size Fractions in the SWIR

The mixing of the calcite with the dolomite in this study is analysed in order to identify the characteristic absorption features of the minerals mixtures spectral reflectance in the SWIR region between 2.164 and 2.653 μm. The synthetic samples with five different compositions of the mineral contents for each type of grain size fraction are composed based on the weight percentage of each mineral in the total weight of the sample (Appendix II). Figure 4.9 shows the position of absorption band as a function of calcite content in the synthetic samples for each grain size fractions. The graphs reveal that there is a significant shift in the position of absorption band for both features due to different calcite contents in the samples. The positions of the carbonate minerals absorption band are centred within the range of 2.32-2.34 μm for the first feature and 2.51-2.54 μm for the second feature. These ratios indicate the alteration process from pure calcite to pure dolomite and these calcite-dolomite ratios could be used as a preliminary proxy to predict the dolomitization patterns in the carbonate rocks or limestone. Therefore, it can be

concluded that the exact positions of the calcite and dolomite absorption band in the SWIR region depend on the amount of mineral contents in the sample.

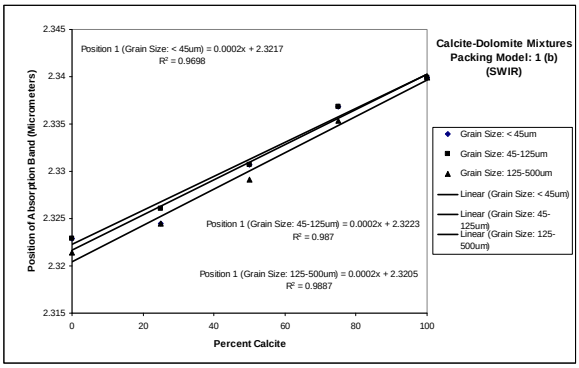

(a)

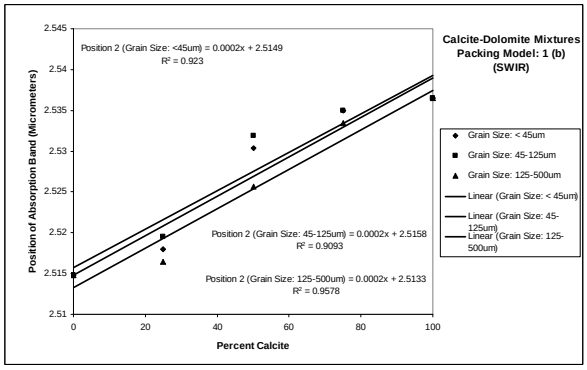

(b)

Figure 4.9. The position of absorption band versus calcite contents in the samples of the calcite-dolomite mixtures for the first (a) and the second feature (b) in the SWIR region.

Furthermore, the graphs showing the detail of position, depth, width, and asymmetry of the carbonate minerals absorption features in the SWIR as a function of the weight percentage of the calcite in the synthetic samples are provided in the Appendix VII. The graphs describe that the depth and width of absorption band vary slightly with calcite contents in the samples. In general, the depth of absorption band for both features increase slightly with increasing the amount of calcite contents in the samples, whereas the width of absorption band decreases slightly with increasing the weight percentage of the calcite in the samples. However, the asymmetry of

absorption band is nearly invariant with the calcite contents in the samples. The asymmetries of both absorption features tend strongly skewed to longer wavelength.

The result of absorption features are also analysed in terms of the calcite and dolomite mixtures with different grain size fractions and the same weight percentage of each mineral contents (Appendix VII). The result indicates that the position of absorption features of the mineral mixtures for both features are varied or shifted slightly by the mixing of the calcite and dolomite with different grain size fractions. One of the most interesting aspects of the mixing between the calcite and dolomite with different grain size fractions is the position of the carbonate minerals absorption band. In this case if the mixing of the calcite and dolomite between fine and coarse grain size fractions is performed, the positions of absorption band in the reflectance spectra of the samples tend moderately to the position of absorption band of the mineral having finer grain size fractions. It may be caused by hiding of the coarse grain size fractions under the fine grain size fraction when the mixing and packing of the samples are prepared. This may happen because the fine grain size fractions are lighter physically than the coarse grain size fractions.

Therefore, the difference in the carbonate mineral contents and grain size fractions influence significantly the absorption features of the calcite-dolomite mixtures and the positions of absorption band shift from the pure dolomite to the pure calcite. The calcite-dolomite ratios of the diagnostic absorption features of the synthetic samples with different mineral contents in the SWIR are centred within the range of 2.32-2.34 μm for the first feature and 2.51-2.54 μm for the second feature. It proves that the absorption features of calcite and dolomite mixtures reflectance spectra are determined by the amount of calcite and dolomite composing the sample and the position of absorption band is nearly linear to the calcite content in the sample, but the ratios slightly change from the previous study as observed by Van der Meer (1995). Moreover, the spectral features also indicate that there is a significant increase in the depth of absorption band when the coarse grain size fractions involve in the mixing of moura calcite marble and chemical pure dolomite.

4.1.5. Absorption Features of the Calcite and Dolomite Mixtures with Different Mineral Contents and Grain Size Fractions in the TIR

In this section, the mixing of the calcite with dolomite is investigated in order to analyse the characteristic absorption features of the minerals mixtures spectra in the TIR region between 10.8900 and 14.8083 μm. This research used the same synthetic samples of the calcite-dolomite mixtures as mentioned in the previous section. Figure 4.10 illustrates the position of absorption band as a function of calcite content

in the synthetic samples for each grain size fractions. The graphs represent that the positions of absorption wavelength for both features not only vary with the calcite contents in the samples, but also vary with the grain size fractions. The positions of the minerals absorption band are centred within the range of wavelengths from pure dolomite to pure calcite as shown in Table 4.1. These positions of absorption band could be used as a preliminary proxy to predict the dolomitization pattern in the carbonate rock or limestone using the TIR band. So it can be concluded that the exact positions of the calcite and dolomite absorption band in the TIR region depend on the amount of mineral contents and grain size fractions in the sample.

Table 4.1. The positions of absorption features of the calcite-dolomite mixture with different mineral contents for each grain size fractions.

No	Grain Size Fractions (µm)	Absorption Features	
		Position 1 (µm)	Position 2 (µm)
1	< 45	11.41 – 11.46	13.65 – 14.01
2	45 – 125	11.42 – 11.50	13.61 – 13.98
3	125 – 500	11.70 – 11.78	13.56 – 13.94

Moreover, the graphs showing the detail of position, depth, width, and asymmetry of the carbonate mineral absorption features as a function of the weight percentage of the calcite in the synthetic samples are provided in the Appendix VIII. The graphs describe that the depth, width, and asymmetry of absorption band vary slightly with the calcite contents in the samples. Generally, the depths of absorption band for both features increase slightly with increasing the amount of calcite contents in the samples as well as width of the first absorption feature. In contrast, the width of the second absorption feature decreases slightly with increasing the weight percentage of the calcite in the samples. In addition, there is a slight increase in asymmetry of absorption band with calcite content in the samples. The asymmetries of both absorption features tend weakly skewed to longer wavelength.

The result of absorption features are also analysed in terms of the calcite and dolomite mixtures with different grain size fractions and the same weight percentage of each mineral contents (Appendix VIII). The result indicates that the positions of absorption band of the minerals for both features are varied slightly by the mixing of the calcite and dolomite with different grain size fractions. The phenomena of hiding the coarse grain size under the fine grain size fraction also occur in the TIR. It is indicated by the positions of absorption band in the reflectance spectra of the

samples tend fairly to the position of absorption band of the mineral having finer grain size fractions.

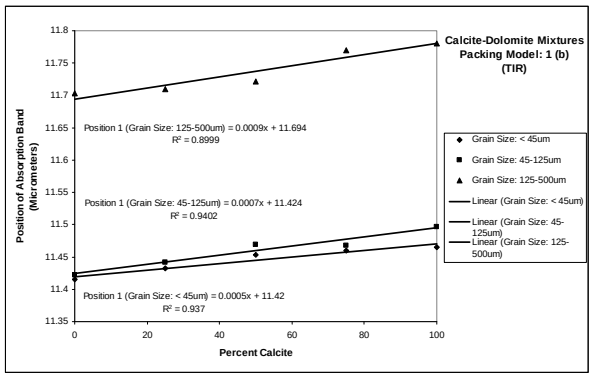

(a)

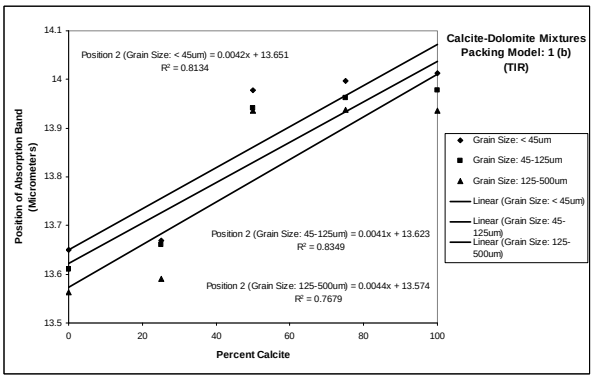

(b)

Figure 4.10. The positions of absorption band versus calcite contents in the samples of the calcite-dolomite mixtures for the first (a) and the second feature (b) in the TIR region.

As a result, the exact positions of the calcite and dolomite absorption band in the TIR region depend on the amount of mineral contents and grain size fractions in the sample and the positions of absorption band shift from the pure dolomite to the pure calcite. The calcite-dolomite ratios of the diagnostic absorption features of the synthetic samples with different mineral contents in the TIR are also dependent on the amount of mineral contents and grain size fractions in the sample.

4.2. Absorption Features of Field Samples in the SWIR

Reflectance spectra of the field or rock samples collected along the two transects of the Bédarieux dolomite mine, southeastern France in the SWIR region between 1.0011 and 2.6526 µm are shown in Figure 4.11. These spectra, based on the literature review of absorption features in the SWIR, illustrate that the strongest vibrational absorption features of the carbonate minerals occur around 2.30-2.34 µm for the first feature (Figure 4.11 (1)) and 2.50-2.55 µm for the second feature (Figure 4.11 (2)). It indicates that the majority of rock samples were formed by carbonate minerals except sample 37 (BMP37) which is a bauxite rock. However, the absorption feature around 0.9 µm due to the presence of iron in the rock can not be identified, because the wavelength range of the spectra that have been recorded is greater than 1.0 µm. The occurrence of carbonate minerals in the rocks can also be recognized from a weak absorption feature in the range of 2.14-2.16 µm.

Moreover, it is obvious from the graph that the another strong vibrational absorption feature is at 1.9 µm due to the presence of combination between hydroxyl and water in the rocks and a diagnostic vibrational spectrum at 1.4 µm specifies an existence of overtone hydroxyl in the rock. These spectral features, especially the spectra of BMP13, 31, 35 and 37, also reveal the position of absorption band at 2.2 µm which symbolise the presence of clay mineral in the rock due to weathering process and it indicates that there are some abandoned mines within the study area.

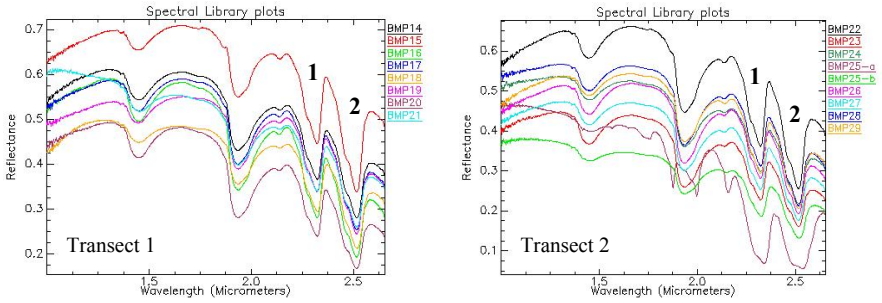

Figure 4.11. Reflectance spectra of the rock samples collected from the western transect (transect 1) and the eastern transect (transect 2) of the dolomite mine in the Bédarieux mining area, southeastern France.

The diagnostic carbonate absorption features of the rock samples reflectance spectra in this research are analysed in order to identify mineral contents and the purity level of the carbonate rocks. It can be used as a preliminary proxy for assessing dolomitization patterns in the study area. The spectra are also used to estimate

natural grain size fractions of the rock samples collected from various locations in the area between Bédarieux and Mourèze as compared to the synthetic samples. The rock samples, as mentioned previously based on the diagnostic absorption features, contain carbonate minerals, especially calcite and dolomite except BMP37 which is a bauxite rock. The occurrence of carbonate minerals in the rock samples are specified by the strong absorption features of the reflectance spectra at about 2.30-2.35 µm and 2.50-2.55 µm, but kind of mineral contents, the purity level and natural grain size fractions of the carbonate rocks can be derived from the precise position of absorption band of the reflectance spectra in the SWIR region as illustrated in the Figure 4.12.

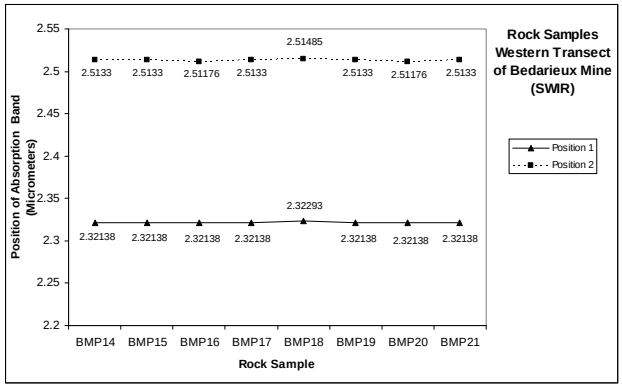

Figure 4.12. The positions of absorption band of the rock samples along the transect 1 of the Bédarieux dolomite mine.

Figure 4.12 shows that the exact positions of absorption band are approximately 2.32 µm for the first feature and 2.51 µm for the second feature, even if the second position of absorption band of the carbonate rocks reflectance spectra vary slightly with the locations of the rock samples collection. These diagnostic positions of absorption band indicate that the rock samples from the western transect of the Bédarieux dolomite mine are pure dolomite rocks. It is also obvious that natural grain size fractions of the rock samples may be nearly between 125 and 500 µm as compared to the synthetic samples of the chemical pure dolomite with different grain size fractions as represented in the Appendix IX.

Moreover, Figure 4.13 reveals that there is a significant shift in the positions of absorption band for both features due to different calcite or dolomite contents in the rock samples. The positions of absorption band of the rocks are centred in the range of 2.32-2.34 µm for the first feature and 2.51-2.53 µm for the second feature. These

ratios indicate the alteration process from nearly pure calcite to pure dolomite and the calcite-dolomite ratios could be used as a preliminary proxy to predict the dolomitization patterns in the study area. The exact positions of absorption band specify that the majority of rock samples are pure dolomite rocks and only a few of the rocks are calcite-dolomite mixtures rocks depending on the locations of the rock samples collection except BMP37, particularly for the rock sample 25. It shows that the positions of absorption band differ from one side (BMP25-a) to another side (BMP25-b) of the rock. The rock sample 25-a is indicated as a calcite and dolomite mixture rock with percentage of the mineral contents are approximately 80% calcite and 20% dolomite as compared to the mixture synthetic samples with grain size fraction in the range of 125-500 µm (Appendix IX). It also clear from the result that the natural grain size fractions of the rock samples may be roughly between 125 µm and 500 µm.

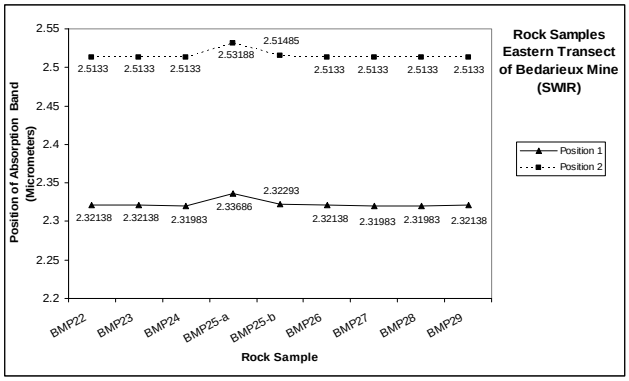

Figure 4.13. The positions of absorption wavelength of the rock samples along the transect 2 of the Bédarieux dolomite mine.

4.3. Calcite and Dolomite Mapping of The HyMap Data

The continuum removal spectrum of carbonate feature derived from the HyMap2003 images has been used for mapping calcite and dolomite using "simple linear interpolation method" (Van der Meer, 2004; 2006b). The carbonate absorption features are derived from the HyMap band 109 centred at 2.2060 µm (shoulder 2) and HyMap band 118 centred at 2.3570 µm (shoulder 1) and two bands as absorption points for interpolation such as the HyMap band 112 centred at 2.2580 µm (absorption point 2) and HyMap band 117 centred at 2.3410 µm (absorption point 1). The classifying and resulting images based on absorption features are shown in Figure 4.14.

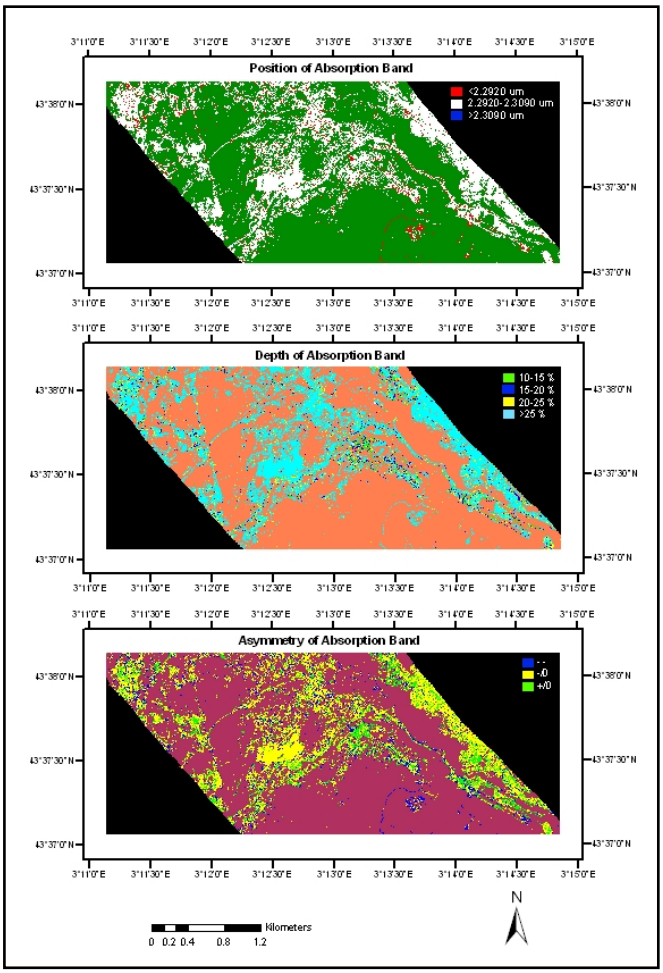

Figure 4.14. Carbonate absorption features: (A) position of absorption band, (B) depth of absorption band (in percentage reflectance relative to the continuum), and (C) asymmetry of absorption band ((--) strongly skewed to shorter wavelength, (-/0) weakly skewed to shorter wavelength, and (+/0) weakly skewed to longer wavelength).

The mapping results of the HyMap2003 images show that carbonate absorption band position is centred in the range of 2.2920-2.3090 µm, where theoretical position of absorption band of pure dolomite is 2.30 µm (Van der Meer, 1994; 1995) and position of absorption band of pure calcite is 2.34 µm (Gaffey, 1986; 1987; Van der Meer, 1994; 1995). These positions illustrate that the majority of abundance rocks or minerals in the study area are dominated by dolomite, although a few of rocks along

the second transects in the Bédarieux dolomite mine, based on the absorption band position of laboratory spectra, indicate calcite and dolomite mixture rocks. The exact position of absorption band depends on the calcite and dolomite contents in the rock. The depth of absorption band of the carbonate minerals tend to greater than 25% of reflectance relative to the continuum. The asymmetry of absorption band of carbonate rocks shifts from weakly skewed to shorter wavelength to weakly skewed to longer wavelength.

The mapping results of carbonate rock absorption features using "simple linear interpolation method" (Van der Meer, 2004; 2006b) indicate that the HyMap airborne hyperspectral data are fairly accurate to identify dolomite, but less accurate or sensitive to map calcite and dolomite mixtures in order to assess dolomitization patterns in the study area. This may be due to the limitations of spectral and spatial resolution or observation scale of the HyMap images as compared to the laboratory spectra. The dolomitization patterns could be estimated in the study area theoretically, because the positions of absorption features of laboratory spectra of the rock samples, especially the rock samples collected along the second transects in the Bédarieux dolomite mine, reveal that the alteration processes of calcite into dolomite occur in the study area. It is indicated by calcite-dolomite ratio of the rock sample in the range of 2.32-2.34 μm for the first feature and 2.51-2.53 μm for the second feature from the pure dolomite to pure calcite.

4.4. Validation

The accuracy of mapping results of the HyMap images, which indicate the presence of calcite and dolomite in the study area, is assessed using the ground truth data or the absorption features of field sample laboratory spectra collected along the two transects of the Bédarieux dolomite mine. The validation process only compares the feature values of classified image pixels corresponding to the locations of field sampling points with the absorption features of field laboratory spectra.

The results as represented in the Appendix X show the position of absorption band of the carbonate rocks derived from laboratory spectra and HyMap2003 spectra along the two transects. These absorption features describe a significance shift in the position of absorption band between laboratory spectra and HyMap2003 spectra. It may be due to differences in the spectral resolutions and spatial resolution or observation scale between the HyMap image and laboratory data. The variability of absorption band position can be seen from the appendix that the rock sample 25-a (BMP25-a) has absorption band position of laboratory spectra at 2.33686 μm,

whereas the rock spectra picked up from the same location in the HyMap image has absorption band position at 2.3090 µm. the laboratory spectra specify that BMP25-a is a calcite-dolomite mixtures rock with percentage of the mineral contents are approximately 80% calcite and 20% dolomite mineral. It is also obvious from the appendix that most of laboratory absorption band position of the rock samples along the two transects are centred at 2.32138 µm, while the image absorption band position of the rocks derived from the same locations are centred at 2.3090 µm.

Figure 4.15 represents absorption band position of the classified image values and types of minerals that are available in the rock samples based on absorption band position of laboratory spectra. The absorption band positions of classified image pixels overlaid with laboratory data of the rocks show that the absorption band positions illustrated on the map indicate dolomite mineral abundance on the study area. These results also represent that some of the classified pixels in the HyMap image can not identify the presence of minerals along the two transect, particularly calcite occurred in the sample 25-a. So the dolomitization patterns on the study area are weakly identified by the HyMap images. For some reason it may be most of the rocks existed in the Bédarieux mining area are pure dolomite.

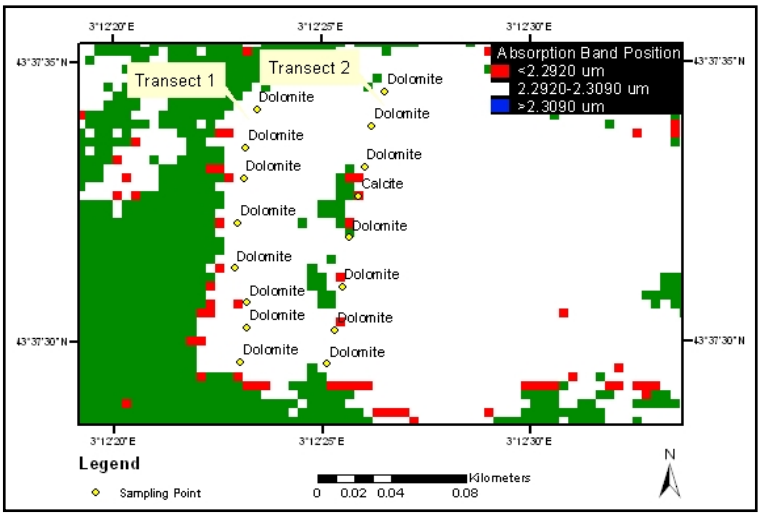

Figure 4.15. Absorption band position of the classified image versus types of minerals in the rock samples derived from absorption band position of the rock laboratory spectra.

5. Discussion

This chapter will be discussing the results and effects of various physical and chemical parameters such as grain size fractions, packing models, and mineral contents on the absorption features of the synthetic samples reflectance spectra of the powdered moura calcite marble and chemical pure dolomite in the SWIR and TIR region. The outcome of the diagnostic absorption features of field sample reflectance spectra in the SWIR and calcite-dolomite mapping from the HyMap imagery using simple linear interpolation method based on the diagnostic absorption features of the carbonate minerals are also being discussed.

5.1. Effects of Grain Size Fractions on Absorption Features of Pure Powdered Calcite and Dolomite Spectra in the SWIR and TIR.

In general, the grain size fractions effects influenced absorption features of reflectance spectra of the pure powdered moura calcite marble and chemical pure dolomite, particularly depth of absorption band and overall brightness of the minerals as stated by Crowley (1986), Gaffey (1986), Salisbury *et al*. (1987), and Van der Meer (1994, 1995). The coarse grain size fractions absorbed more electromagnetic radiation than the fine grain size fractions due to brightness factors (Gaffey, 1986; Van der Meer, 1994; 1995) and internal optical path (Clark and Roush, 1984). The fine grain size fractions of the mineral were brighter and shorter internal optical path than the coarse grain size so it absorbed less electromagnetic energy that penetrate to the surface of the minerals.

The positions of absorption band for both features of the calcite were invariant with grain size fractions. The diagnostic positions of absorption band of the calcite in the SWIR were centred at 2.34 μm and 2.5365 μm. These absorption wavelength positions were caused by vibrational absorption of carbonate ion (CO_3^{-2}). Moreover, the dolomite has a slight difference in absorption band position due to grain size fraction effects in the SWIR. The fine grain size fraction in the range of 45-125 μm tended to centred at 2.32293 μm and 2.51485 μm and the coarse grain size fractions between 125 and 500 μm occurred at 2.32138 μm and 2.5133 μm. The changing position of absorption band of the dolomite in term of different grain size fractions in the SWIR might be caused by the amount of Mg in the sample as stated by Gaffey (1985) that chemical composition will influence position of absorption band. The

coarse grain size fractions were probably content more Mg than the fine grain size fractions. The presence of Mg in carbonate mineral influenced slightly position of absorption band of the dolomite. The occurrences of vibratonal absorption features at these diagnostic wavelengths were also caused by carbonate ion in the dolomite. It can be concluded that the positions of absorption band of the moura calcite marble and chemical pure dolomite in the SWIR changed slightly as compared to previous study reported by Hunt and Salisbury (1971), Gaffey (1986, 1987), and Van der Meer (1994).

However, the absorption band positions of the calcite and dolomite in the TIR were dependent on grain size fractions in the sample. The diagnostic positions of absorption band of the calcite in the TIR were around 11.45–11.75 μm and 14.00–13.92 μm. In addition, the diagnostic positions of absorption band of the dolomite in the TIR were around 11.42–11.67 μm and 13.65–13.44 μm. The shifting of absorption band positions might be caused by the bending vibrational absorption of the carbonate ion as stated by Salisbury *et al*. (1987). The bending vibrational processes might be influenced by the amount of carbonate ion in the grain of the minerals, where the coarse grain size were probably content more carbonate ion than the fine grain size. So the coarse grain size tended to have strong bending vibrational absorption when it interacted with electromagnetic radiation. These absorption band positions also changed slightly as compared to previous result observed by Huang and Kerr (1960) and Reig *et al*. (2002).

5.2. Effects of Packing Models on of Pure Powdered Calcite and Dolomite Spectra in SWIR.

Absorption features of reflectance spectra of moura calcite marble and chemical pure dolomite were insignificantly influenced by the packing models. Packing or porosity of the synthetic samples only affected the depth of absorption band of the minerals spectra. Positions of absorption band of both the minerals were invariant with packing models. Where loosely stacked packing samples were marginally deeper spectral absorption than compact packing samples or the depths of absorption band decrease slightly with increasing the compact of packing models (Gaffey, 1986). It might be caused by the smoothness or texture of the sample surface. The loosely stacked packing sample seems rougher surface than compact packing sample so it absorbs more electromagnetic radiation. The compact packing sample seemed brighter due to flat and compact grain surface so it reflected more electromagnetic energy when photons radiated the compact grain surface.

5.3. Effects of Different Mineral Contents and Grain Size Fractions on Absorption Features of Calcite-Dolomite Mixture Spectra in the SWIR and TIR.

Absorption features of the synthetic samples in the SWIR and TIR were determined substantially by the difference in mineral contents and grain size fractions of the calcite-dolomite mixtures in the synthetic samples. The most significance absorption parameter that was influenced by the differences in mineral contents and grain size fractions was position of absorption band. The positions of absorption band shifted from the pure dolomite to the pure calcite and the calcite-dolomite ratios of the diagnostic absorption features of the synthetic samples with different mineral contents in the SWIR were centred within the range of 2.32-2.34 μm and 2.51-2.54 μm. The calcite-dolomite ratios of the diagnostic absorption features of the synthetic samples with different mineral contents in the TIR were also dependent on the amount of mineral contents and grain size fractions in the sample (Table 4.1). These ratios can be used as a preliminary proxy to assess dolomitization patterns.

In terms of calcite-dolomite mixtures with different grain size fractions in the SWIR and TIR, the positions of absorption band were controlled by the fine grain size fractions in the samples. It might be caused by hiding of the coarse grain size fractions under the fine grain size fraction when the mixing and packing of the samples were prepared due to the fine grain size are lighter physically than the coarse grain size. It proved that the absorption features of calcite and dolomite mixtures reflectance spectra were determined by the amount of calcite and dolomite composing the sample. The position of absorption band is nearly linear to the calcite content in the sample, but the ratios slightly changed from the previous study as observed by Van der Meer (1995). Moreover, the spectral features also indicated that there was a significant increase in the depth of absorption band when the coarse grain size fractions involved in the mixing of moura calcite marble and chemical pure dolomite.

5.4. Absorption Feature Characteristics of Field Samples Spectra in the SWIR

The diagnostic absorption features of the field sample spectra in the SWIR indicated that the majority of the field samples collected in the area between Bédarieux and Mourèze, southeastern France are dolomite. It was proved by the positions of absorption band which were exactly same as the synthetic sample of chemical pure dolomite. There were also some field samples collected along transect 2 of the Bédarieux dolomite mine are calcite and dolomite mixtures. These diagnostic

positions of absorption band indicated that the alteration process from nearly pure calcite to pure dolomite occurred in the Bédarieux mine and the calcite-dolomite ratios of field samples spectra could be used as a preliminary proxy to predict the dolomitization patterns in the study area. In addition, the absorption band positions also indicated that natural grain size fractions of the rock samples may be nearly between 125 and 500 μm as compared to the synthetic samples of the pure dolomite.

5.5. Characterisation of the HyMap Images as a Proxy for Assessing Dolomitization Patterns

The calcite-dolomite mapping results of the HyMap2003 images using simple linear interpolation method show that the majority of abundance rocks or minerals in the study area are dominated by dolomite. The results also indicated that the HyMap airborne hyperspectral data were fairly accurate to identify dolomite, but less accurate or sensitive to map calcite and dolomite mixtures in order to assess dolomitization patterns in the study area. It may be due to the limitations of spectral (Figure 4.16) and spatial resolution or observation scale of the HyMap images as compared to the laboratory spectra. The dolomitization patterns could be estimated in the study area theoretically, because the positions of absorption features of laboratory reflectance spectra of the rock samples, especially a few of rock samples collected along the eastern transects of the Bédarieux dolomite mine, revealed that the alteration processes of calcite into dolomite occurred in the study area. So the dolomitization patterns on the study area were weakly identified by the HyMap images desired refinements, but the simple linear interpolation method based on spectral absorption feature parameters revealed a greatly potential to map calcite and dolomite. For some reason it may be most of the rocks existed in the Bédarieux mining area are pure dolomite.

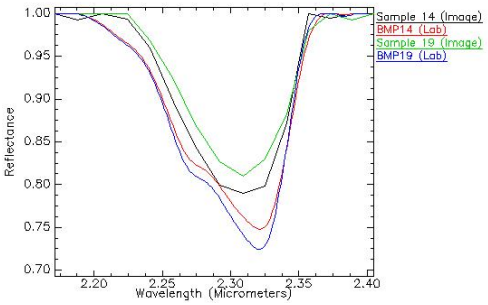

Figure 4.16. Shifting absorption band position between laboratory spectra and HyMap2003 spectra corresponding to the locations of field sampling points due to different spectral resolution.

6. Conclusion and Recommendation

6.1. Conclusion

- The differences in grain size fractions and packing models only influenced significantly the depths of absorption bands of reflectance spectra of the pure powdered moura calcite marble and chemical pure dolomite in the SWIR.
- Pure moura calcite marble has two characteristic positions of absorption band in the SWIR centred at 2.34 μm and 2.5365 μm.
- Chemical pure dolomite has a slight difference in absorption band position due to grain size fraction effects in the SWIR. The fine grain size fraction in the range of 45-125 μm tended to centred at 2.32293 μm and 2.51485 μm and the coarse grain size fractions between 125 and 500 μm occurred at 2.32138 μm and 2.5133 μm.
- Absorption band positions of the calcite and dolomite in the TIR were dependent on grain size fractions in the sample. The diagnostic positions of absorption band of the calcite in the TIR were around 11.45–11.75 μm and 14.00–13.92 μm. While the diagnostic positions of absorption band of the dolomite were around 11.42–11.67 μm and 13.65–13.44 μm.
- Position of absorption band of the calcite and dolomite mixtures reflectance spectra in the SWIR and TIR were determined by the amount of calcite and dolomite composing the sample. The position of absorption band is nearly linear to the calcite content in the sample.
- The diagnostic absorption feature of the calcite-dolomite mixture in SWIR derived calcite-dolomite ratio within the range of 2.32-2.34 μm and 2.51-2.54 μm from pure dolomite to pure calcite. The TIR spectra of the calcite-dolomite mixtures depended on the amount of mineral contents and grain size fractions in the sample. These ratios can be used as a preliminary proxy for assessing dolomitization patterns.
- The diagnostic absorption features of the field sample spectra in the SWIR indicated that the majority of the field samples collected in the area between Bédarieux and Mourèze, southeastern France are dolomite and a few of rocks are calcite-dolomite mixture.
- The results of calcite-dolomite mapping of the HyMap2003 images using simple linear interpolation method showed that the majority of abundance rocks or minerals in the study area are dominated by dolomite.

- The HyMap airborne hyperspectral data were fairly accurate to identify dolomite, but less accurate or sensitive to map calcite and dolomite mixtures which are a proxy for assessing dolomitization patterns in the study area.
- The dolomitization patterns in the study area were weakly identified by the HyMap images as compare to the laboratory reflectance spectra of the field samples, but the simple linear interpolation method based on spectral absorption feature parameters revealed a greatly potential to map calcite and dolomite.

6.2. Recommendation

- X-ray diffraction analysis and hydrochloric acid dilution test would be necessary to derive chemical composition and purity level of synthetic and field samples. These data could be used to analyse the effects of mineral mixtures and chemical composition on absorption features of synthetic and field samples.
- Packing and mixing synthetic sample should be done using standard equipment in order to obtain the same homogeneous and compact synthetic samples.
- Calcite-dolomite ratio derived from synthetic samples spectra in the SWIR and TIR could be used to refine spectral sampling interval or spectral resolution of HyMap images.
- Using other hyperspectral imagery such as AVIRIS and DAIS may provide a great probability to assess dolomitization patterns in the study area.
- The real ground truth data of reflectance spectra of the rocks would be essential to collect from the study area in order to validate the HyMap images.

References

Berner, R. A. 1965. Dolomitization of Mid-Pacific Atolls. *Science, New Series*, 147 (3663), 1297-1299.

Bertaux, J., Froehlich, F., and Ildefonse, P., 1998. Multicomponent analysis of FTIR spectra; quantification of amorphous and crystallized mineral phases in synthetic and natural sediments. Journal of Sedimentary Research, 68(3):440-447.

Bierwirth, P., Huston, D., and Blewett, R. 2002. Hyperspectral mapping of mineral assemblages associated with gold mineralization in the Central Pilbara, Western Australia. *Economic Geology*, 97, 819–826.

Bissell, H. J. and Chilingar, G. V. 1967. *Classification of Sedimentary Carbonate Rocks*. *In*: Chilingar, G. V., Bissell, H. J., and Fairbridge, R. W. (Eds.), *Carbonate Rocks: Developments in Sedimentology*, 9A. Elsevier, Amsterdam, pp. 87-168.

Campbell, J. B. 1996. *Introduction to Remote Sensing*. 2nd ed., Taylor and Francis Ltd, London.

Clark, R. N., and Roush, T. L. 1984. Reflectance spectroscopy: Quantitative analysis techniques for remote sensing applications. *Journal of Geophysical Research*, 89 (B7), 6329−6340.

Clark, 1999. *Spectroscopy of Rock and Minerals and Principles of Spectroscopy*. *In*: Rencz, A. N. (Ed.), *Remote Sensing for the Earth Sciences: Manual of Remote Sensin.* 3thed.,vol.3, John Wiley & Sons, New York, pp. 3-58.

Cocks, T., Jenssen, R., Stewart, A., Wilson, I., and Shields, T. 1998. The HyMAP™ airborne hyperspectral sensor: The system, calibration and performance. *First EARSel Workshop on Imaging Spectroscopy*, Zurich.

Crowley, J. K. 1986. Visible and near-infrared spectra of carbonate rocks: Reflectance variations related to petrographic texture and impurities: *Journal of Geophysical Research*, 91 (B5), 5001-5012.

Dietrich, R. V. and Skinner, B. J. 1979. *Rocks and Rock Minerals*. John Wiley & Sons, New York.

Friedman, G. M. and Sanders, J. E. 1967. *Origin and Occurrence of Dolostones*. *In*: Chilingar, G. V., Bissell, H. J., and Fairbridge, R. W. (Eds.), *Carbonate Rocks: Developments in Sedimentology*, 9A. Elsevier, Amsterdam, pp. 266-348.

Gaffey, S. J. 1985. Reflectance spectroscopy in the visible and near infrared (0.35-2.55 microns): Applications in carbonate petrology. *Geology*, 13, 270-273.

Gaffey, S. J. 1986. Spectral reflectance of carbonate minerals in the visible and near-infrared (0.35-2.55 microns): Calcite, aragonite, and dolomite. *American Mineralogist*, 71, 151-162.

Gaffey, S. J. 1987. Spectral reflectance of carbonate minerals in the visible and near-infrared (0.35-2.55 microns): Anhydrous carbonate minerals. *Journal of Geophysical Research*, 92 (B2), 1429-1440.

Gaffey, S. J., McFadden, L. A., Nash, D., and Pieters, C. M. 1997. *Ultraviolet, Visible, and Near-Infrared Reflectance Spectroscopy: Laboratory Spectra of Geologic Materials*. *In*: Pieters, C. M. and Englert, P. A. J. (Eds.), *Remote Geochemical Analysis: Elemental and Mineralogical Composition*. Cambridge University Press, Cambridge, pp. 43-78.

Gèze, B. 1979. Languedoc méditerranéen, Montagne Noire, Guides Géologiques Régionaux, Masson.

Goetz, A. F. H. 1991. Imaging spectrometry for studying Earth, Air, Fire and Water. *EARSeL Advance in Remote Sensing* 1, 3-15.

Griffiths, P. R. and De Haseth, J. A. 2007. *Fourier Transform Infrared Spectrometry*. 2nd ed., John Wiley & Sons, New Jersey.

Gupta, R. P., 2003. *Remote Sensing Geology*. 2nd ed., Springer, Heidelberg.

Hamilton, W. R., Woolley, A. R., and Bishop, A. C. 1995. *Hamlyn Guide: Minerals, Rocks and Fossils*. Mandarin Offset, Hong Kong.

Harbaugh, J. W. 1967. *Carbonate Oil Reservoir Rock*. *In*: Chilingar, G. V., Bissell, H. J., and Fairbridge, R. W. (Eds.), *Carbonate Rocks: Developments in Sedimentology*, 9A. Elsevier, Amsterdam, pp. 349-398.

Hatch, F. H. and Rastall, R. H. 1965. *Textbook of Petrology: Petrology of the Sedimentary Rocks*. Vol. 2. Thomas Murby & Co. London.

Huang, C. K. and Kerr, P. F. 1960. Infrared study of the carbonate minerals. *The American Mineralogist*, 45, 311-324.

Hunt, G. R. and Salisbury, J. W. 1971. Visible and near infrared spectra of minerals and rocks: II. Carbonates. *Modern Geology*, 2, 23-30.

Hunt, G. R. 1977. Spectral signatures of particulate minerals in the visible and near-infrared. *Geophysics*, 42, 501–513.

Hunt, G. R. 1982. *Spectroscopic Properties of Rocks and Minerals*. *In*: Carmichael, R. S. (Ed.), *Handbook of Physical Properties of Rock*. CRC Press, Boca Raton, Vol. I, pp. 295-385.

Kratt, C., Calvin, W., and Coolbaugh, M. 2006. Geothermal exploration with Hymap hyperspectral data at Brady–Desert Peak, Nevada. *Remote Sensing of Environment*, 104, 313–324.

Kirkaldy, J. F. 1976. *Minerals and Rocks in colour*. Yselpress, Deventer.

Location of Dolomite site, [Online], Available: http://pedagogie.ac-montpellier.fr/svt/litho/carlencas-dolomie/localisation.htm [accessed 01 September 2008].

Mustard, J. F. and Sunshine, J. M. 1999. *Spectral Analysis for Earth Science: Investigations Using Remote Sensing Data*. *In*: Rencz, A. N. (Ed.), *Remote Sensing for the Earth Sciences: Manual of Remote Sensin.* 3th ed.,vol.3, John Wiley & Sons, New York, pp. 251-306.

Reig, F.B., Adelantado, J.V.G. and Moya Moreno, M.C.M., 2002. FTIR quantitative analysis of calcium carbonate (calcite) and silica (quartz) mixtures using the constant ratio method. Application to geological samples. *Talanta*, 58 (4), 811-821.

Riaza, A., Melendez, E.G., Suarez, M. and Muller, A. 2005. Mineral climate indicators in paleoflooded and emerged areas around lake marshes (Tablas de Daimiel, Spain) using hyperspectral DAIS 7915 spectrometer data. *International Journal of Remote Sensing*, 26 (20), 4565-4582.

Sabins, F. F. 2007. *Remote Sensing: Principles and Interpretation*. 3rd ed., Waveland Press Inc., Long Grove, Illinois.

Salisbury, J. W., Hapke, B., and Eastes, J. W. 1987. Usefulness of weak bands in midinfrared remote sensing of particulate planetary surface. *Journal of Geophysical Research*, 92 (B1), 702-710.

Sluiter, R. 2005. Mediterranean land cover change: Modelling and monitoring natural vegetation using GIS and remote sensing. Dissertation, Utrecht University, the Netherlands.

Van der Meer, F. 1994. Sequential indicator conditional simulation and indicator kriging applied to discrimination of dolomitization in GER 63-channel imaging spectrometer data. *Nonrenewable Resources*, 3, 146–164.

Van der Meer, F. 1995. Spectral reflectance of carbonate mineral mixtures and bidirectional reflectance theory: Quantitative analysis techniques for application in remote sensing. *Remote Sensing Review*, 13, 67–94.

Van der Meer, F. 2004. Analysis of spectral absorption features in hyperspectral imagery. *International Journal of Applied Earth Observation and Geoinformation*, 5, 55–68.

Van der Meer, F. 2006a. The effectiveness of spectral similarity measures for the analysis of hyperspectral imagery. *International Journal of Applied Earth Observation and Geoinformation*, 8, 3–17.

Van der Meer, F. 2006b. Indicator kriging applied to absorption band analysis in hyperspectral imagery: A case study from the Rodalquilar epithermal gold mining area, SE Spain. *International Journal of Applied Earth Observation and Geoinformation*, 8, 61–72.

Van der Meer, F. D. 2006c. *Basic Physics of Spectrometry*. *In*: Van der Meer, F. D. and De Jong, S. M. (Eds.), *Imaging spectrometry: Basic principles and prospective applications.* Springer, Dordrecht, pp.3-16.

Van der Meer, F. D., De Jong, S. M., and Bakker, W. 2006. *Imaging Spectrometry: Basic Analytical Techniques*. *In*: Van der Meer, F. D. and De Jong, S. M. (Eds.), *Imaging spectrometry: Basic principles and prospective applications.* Springer, Dordrecht, pp.17-61.

Van Ruitenbeek, F.J.A., Debba, P., van der Meer, F.D., Cudahy, T., van der Meijde, M., Hale, M. 2006. Mapping white micas and their absorption wavelengths using hyperspectral band ratios. *Remote Sensing of Environment*, 102 (3–4), 211–222.

Van Ruitenbeek, F.J.A., van der Werff, H.M.A., Hein, K.A.A., and van der Meer, F.D. 2008. Detection of pre-defined boundaries between hydrothermal alteration zones using rotation-variant template matching. *Computers and Geosciences,* doi:10.1016/j.cageo.2007.11.001.

Windeler, D.S., and Lyon, R.J.P. 1991. Discriminating dolomitization of marble in the Ludwig Skarn near Yerington, Nevada, using high-resolution airborne infrared imagery. *Photogrammetric Engineering & Remote Sensing*, 57 (9), 1171-1177.

Appendix I

The HyMap operating system and configuration specifications (*Source:* Cocks *et al*., 1998).

Typical Operational Parameters	
Platform	Light, twin-engine aircraft e.g. Cessna 404, unpressurised
Altitudes	2000 – 5000 m AGL
Ground Speeds	110 – 180 km

Spatial Configurations	
IFOV	2.5 mrad along track 2.0 mrad across track
FOV	60 degrees (512 pixels)
Swath	2.3 km at 5 m IFOV (along track) 4.6 km at 10 m IFOV (along track)

Spectral Configurations			
Module	**Spectral Range**	**Bandwidth Across Module**	**Average Spectral Sampling Interval**
VIS	0.45 – 0.89 µm	15 – 16 nm	15 nm
NIR	0.89 – 1.35 µm	15 – 16 nm	15 nm
SWIR1	1.40 – 1.80 µm	15 – 16 nm	13 nm
SWIR2	1.95 – 2.48 µm	18 – 20 nm	17 nm

Appendix II

Synthetic Samples

1. Mixtures of calcite - dolomite with different mineral contents

Table 1. Mixtures of calcite - dolomite (the same grain size fractions: <45μm)

Sample	Calcite		Dolomite		Total
	%	gram	%	gram	gram
I-CD1.01	100	25	0	0	25
I-CD1.02	75	18.75	25	6.25	25
I-CD1.03	50	12.50	50	12.50	25
I-CD1.04	25	6.25	75	18.75	25
I-CD1.05	0	0	100	25	25

Table 2. Mixtures of calcite - dolomite (the same grain size fractions: 45-125μm)

Sample	Calcite		Dolomite		Total
	%	gram	%	gram	gram
I-CD2.01	100	25	0	0	25
I-CD2.02	75	18.75	25	6.25	25
I-CD2.03	50	12.50	50	12.50	25
I-CD2.04	25	6.25	75	18.75	25
I-CD2.05	0	0	100	25	25

Table 3. Mixtures of calcite - dolomite (the same grain size fractions: 125-500μm)

Sample	Calcite		Dolomite		Total
	%	gram	%	gram	gram
I-CD3.01	100	25	0	0	25
I-CD3.02	75	18.75	25	6.25	25
I-CD3.03	50	12.50	50	12.50	25
I-CD3.04	25	6.25	75	18.75	25
I-CD3.05	0	0	100	25	25

2. Mixtures of calcite - dolomite with different grain (particle) size fractions

Table 6. Calcite-dolomite mixtures (the same weight percentage of the minerals total weight)

Sample	Calcite		Dolomite		Total
	particle size (μm)	%	particle size (μm)	%	gram
II-CD1	<45	50	125-500	50	25
II-CD2	45-125	50	45-125	50	25
II-CD3	125-500	50	<45	50	25
II-CD4	<45	50	45-125	50	25
II-CD5	45-125	50	<45	50	25
II-CD6	<45	50	<45	50	25
II-CD7	45-125	50	125-500	50	25
II-CD8	125-500	50	45-125	50	25
II-CD9	125-500	50	125-500	50	25

Appendix III

OPUS-OPERATOR SOFTWARE

SWIR Setting

Measurement and setting of parameters can be started by clicking on symbol "Advance data collection" then measurement window will appear with menu as follow and setting can be conducted :

1. Basic :

Experiment	: Load "Sphere_NIR_Nasrullah.xpm
Operator name	: Administrator
Sample description	: Maura_CalciteMarble_-45
Path	: D:\Nasrullah
File name	: Maura_CalciteMarble_-45
Background single channel	: Reference (on instrument)
Sample single channel	: Sample (on instrument)

2. Advenced :

Experiment	: Load Save '
Sphere_NIR_Nasrullah.xpm	
File name	: <@snm>
Path	: D:\Nasrullah
Resolution	: 16 cm^{-1} (wavenumber)
Sample scan time	: 256 scans (seconds)
Background scan time	: 256 scans
Save data from	: 10000 cm^{-1} to 3000 cm^{-1}

Result spectrum : Reflectance

☐ Additional data treatment

☐ Atmospheric compensation

Interferogram size : 3554 points FT size : 4K

Data blocks to be saved

☐ Reflectance ☐ Phase Spectrum

☐ Single ☐ Background

☐ Sample Interferogram ☐ Background Interferogram

3. Optic

External synchronization	: Off
External source setting	: NIR
External beam splitter	: CaF2
Optical filter setting	: Open
Aperture setting	: 8 mm
Aperture accessory	: any
Measurement channel	: right front exit

This parameter that have been set by mean of OPUS software can be explored in more detail in the appendix 2

Background mean channel	: right front exit
Background detector setting	: InGaAs on sphere (External)
Background preamp gain	: c
Background velocity	: 10 KHz
Sample signal gain	: Automatic
Background signal gain	: Automatic
Delay after device change	: 0 sec
Delay before measurement	: 0 sec
Delay optical bench ready	: OFF

4. Acquisition

Wanted high frequency limit	: 15000	15796.97 cm^{-1}
Wanted low frequency limit	: 0	0.00 cm^{-1}
Wanted laser wave number	: 15796.96	
Interferogram size	: 3554 points	
FTsize : 4k		
High pass filter	: Open	
Low pass filter	: 10 KHz 15797 cm^{-1}	
Acquisition mode	: double sided, Forward_Backward	

Correlation mode : OFF
External analog signal : No analog value

5. FT
Phase relosution : 32 Phase interferogram points : 1777
Phase correlation mode : Mertz
Apodization function : Happ-Genzel
Zerofilling factor : 1

Interferogram size : 3554 points FT size : 4 k

6. Display

☐ Display single scans before measurement

☐ Display during measurement

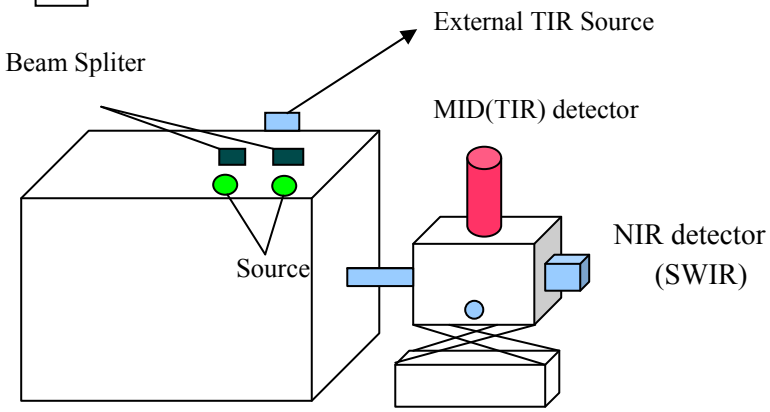

7. Background

Beam splitter
Load Background Detector is saturate of
Too much energy coming

Save Background
Clear background

8. Check Signal
Save peak position
Scale display
Scan range
Show

☐ Store mode

◉ Interferogram

○ Spectrum

○ ADC Count

Amplitude : -13614 (ok)

9. Beam Path
Ready (on) to measure (NIR) :

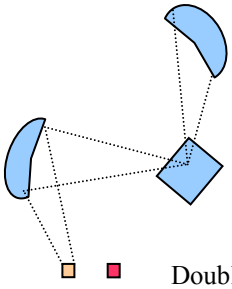

Double click

Double click

10. Spectral Range Selection

Best Source	: NIR	Spectral absorption Maura-Calcite
Best Detector	: Classic Style	Marble at 4273.513 cm^{-1} (wn)
Best Beam splitter	: CAF2	~ 2.34 µm

TIR Setting

Experiment set up same as : Sphere_MCT_Wardana_MSc.XPM

a. Advanced

Experiment Save as : Sphere_MCT_Nasrullah.XPM
File name : <@snm>
Path : D:\Nasrullah\Wavenumber_MIR_PureCalDol

Resolution : 8 cm^{-1} (Wavenumber)
Sample scan time : 4096 scans
Background scan time : 4096 scans
Save data from : 7000 cm^{-1} to 500 cm^{-1}

Result spectrum : Reflectance

☐ Additional data treatment
☐ Atmospheric compensation

Interferogram Size : 7108 points FT size : 8K

Data Block to be saved

√ Reflectance √ Phase Spectrum
√ Single Channel √ Background
√ Sample Interferogram √ Background Interferogram

b. Basic

Experiment : Sphere_MCT_Nasrullah.XPM
Operator name : Administrator
Sample Description : Chemical_Pure Dolomite_-45
Path : D:\Nasrullah\Wavenumber_MIR_Pure CalDol
File name : Chemical_Pure Dolomite_-45

c. Optic

External Synchronisation : OFF
Source Setting : Backward Input
Beam splitter : KBr
Optical Filter Setting : Open

Aperture Setting : 8 mm
Accessory : Any
Measurement Channel : Right Front Exit
Background Measurement Channel : Right Front Exit
Detector Setting : MCT on Sphere (External)
Scanner Velocity : 40 KHz
Preamp gain : Ref

Sample Signal Gain : Automatic
Background Signal Gain : Automatic

Delay after device change : 0 sec
Delay before measurement : 0 sec
Optical bench ready : OFF

d. Acquisition
Same as NIR, only change :
Interferogram size : 7108 points & FTsize : 8K
Lowpass filter : 40 KHz

e. FT
Same as NIR
Zerofilling factor : 1
Amplitude : -5241 ~ - 5200

Appendix IV: Sample locations, Bedarieux – Mourèze Peyne (BMP)

Sample ID	X-UTM WGS84 31T	Y-UTM WGS84 31T	Remarks
North of mine:			
11	516551	4831331	Abandoned mine, bauxite
12	515717	4831605	Abandoned mine, bauxite
13	516008	4829555	Road side D908
Transect 1:			
14	516660	4830373	Sandy, grainy
15	516654	4830352	Sandy, grainy
16	516653	4830335	
17	516650	4830310	Between pine trees (sept.08)
18	516648	4830285	Idem
19	516655	4830266	Hard ridge, in situ
20	516655	4830252	Strongly weathered
21	516651	4830233	Hard ridge, in situ
Transect 2:			
22	516729	4830383	Weather, pulverized rocks
23	516722	4830364	Disturbed
24	516718	4830341	Close to wheel tracks
25	516715	4830325	Mg crystals
26	516710	4830302	Side wall of active quarry
27	516706	4830275	Idem
28	516702	4830251	
29	516698	4830232	Near wheel tracks
Mourèze:			
30	526643	4829544	Sandy, reddish Fe
31	526913	4829482	
32	527027	4829415	Sandy
33	527393	4829245	
34	527902	4829195	
35	528494	4829465	Massive dolomite, not crumpy
Others:			
36	516842	4831123	NE of dolomite mine
37	517490	4828300	Bauxite, mine Carlencas

Appendix V:

Absorption features of reflectance spectra of calcite and dolomite as a function of grain size fractions in the SWIR

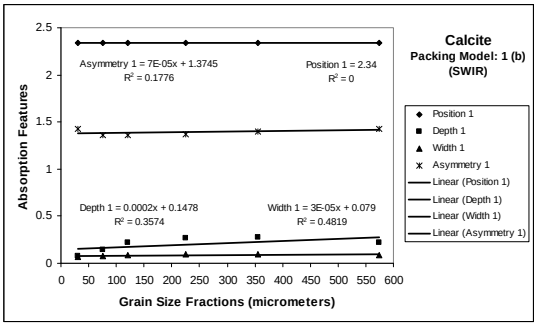

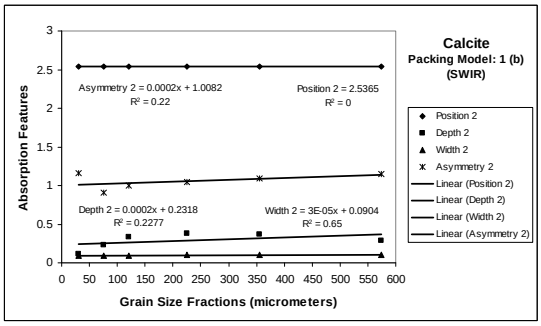

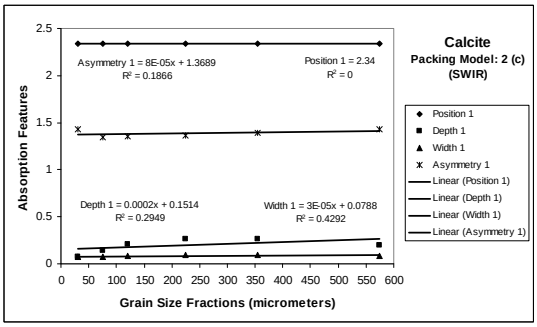

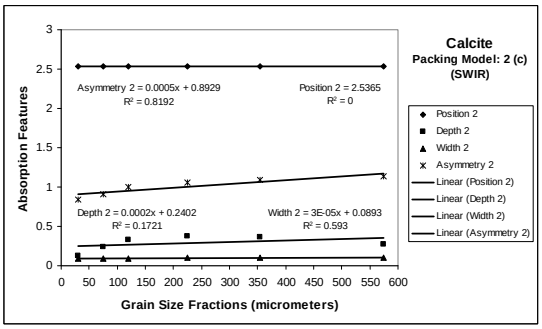

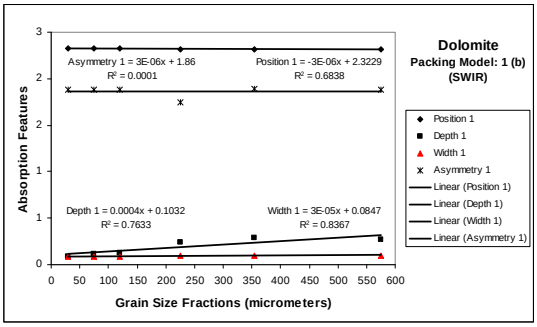
Dolomite
Packing Model: 1 (b)
(SWIR)
Asymmetry 1 = 3E-06x + 1.86
R² = 0.0001
Position 1 = -3E-06x + 2.3229
R² = 0.6838
Depth 1 = 0.0004x + 0.1032
R² = 0.7633
Width 1 = 3E-05x + 0.0847
R² = 0.8367
Position 1
Depth 1
Width 1
Asymmetry 1
Linear (Position 1)
Linear (Depth 1)
Linear (Width 1)
Linear (Asymmetry 1)
Absorption Features
Grain Size Fractions (micrometers)

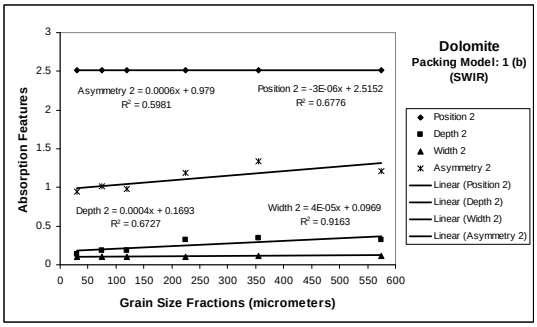
Dolomite
Packing Model: 1 (b)
(SWIR)
Asymmetry 2 = 0.0006x + 0.979
R² = 0.5981
Position 2 = -3E-06x + 2.5152
R² = 0.6776
Depth 2 = 0.0004x + 0.1693
R² = 0.6727
Width 2 = 4E-05x + 0.0969
R² = 0.9163
Position 2
Depth 2
Width 2
Asymmetry 2
Linear (Position 2)
Linear (Depth 2)
Linear (Width 2)
Linear (Asymmetry 2)
Absorption Features
Grain Size Fractions (micrometers)

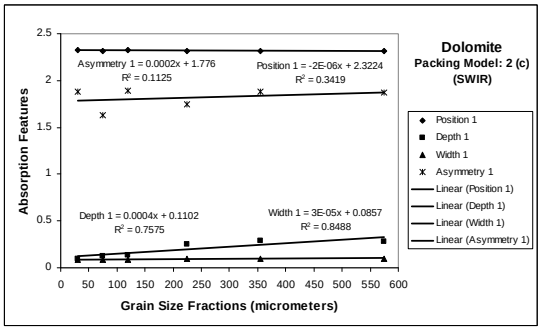
Dolomite
Packing Model: 2 (c)
(SWIR)
Asymmetry 1 = 0.0002x + 1.776
R² = 0.1125
Position 1 = -2E-06x + 2.3224
R² = 0.3419
Depth 1 = 0.0004x + 0.1102
R² = 0.7575
Width 1 = 3E-05x + 0.0857
R² = 0.8488
Position 1
Depth 1
Width 1
Asymmetry 1
Linear (Position 1)
Linear (Depth 1)
Linear (Width 1)
Linear (Asymmetry 1)
Absorption Features
Grain Size Fractions (micrometers)

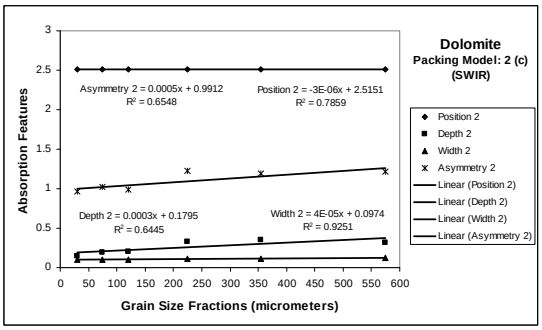
Dolomite
Packing Model: 2 (c)
(SWIR)
Asymmetry 2 = 0.0005x + 0.9912
R² = 0.6548
Position 2 = -3E-06x + 2.5151
R² = 0.7859
Depth 2 = 0.0003x + 0.1795
R² = 0.6445
Width 2 = 4E-05x + 0.0974
R² = 0.9251
Position 2
Depth 2
Width 2
Asymmetry 2
Linear (Position 2)
Linear (Depth 2)
Linear (Width 2)
Linear (Asymmetry 2)
Absorption Features
Grain Size Fractions (micrometers)

Appendix VI

Absorption features of the calcite and dolomite in the TIR

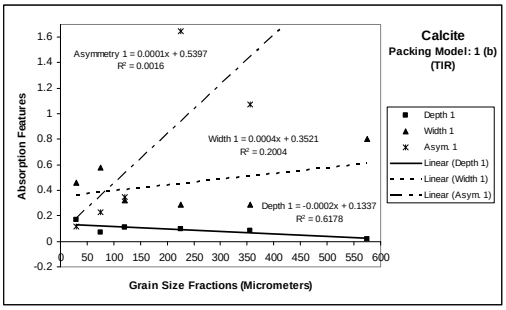

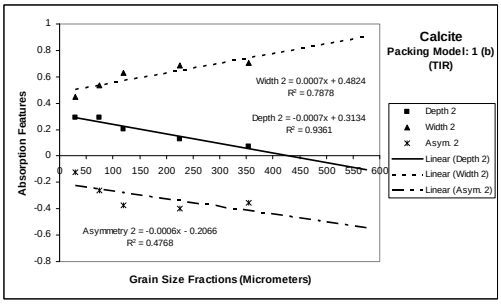

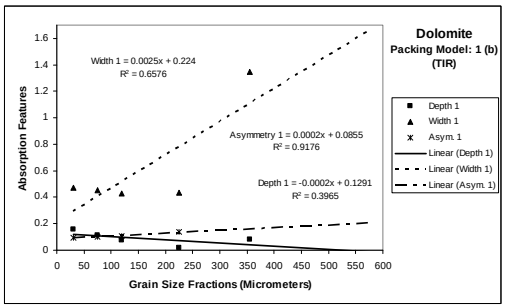

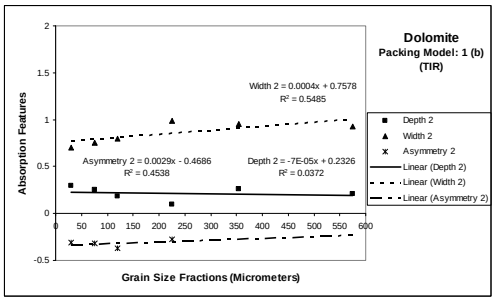

Appendix VII

Absorption features of calcite-dolomite mixture in the SWIR

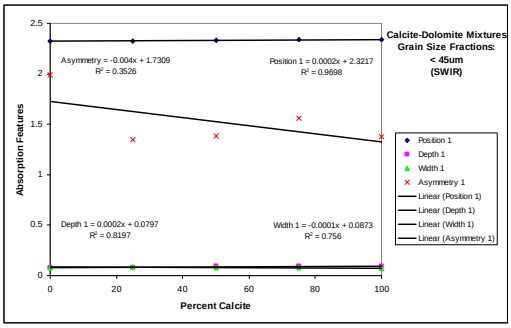

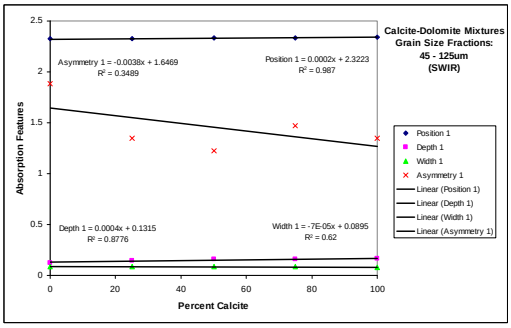

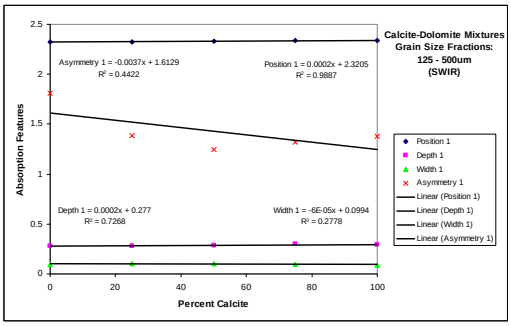

The positions of absorption features of the calcite-dolomite mixture with different grain size fractions and the same weight percentage of the carbonate mineral contents in the SWIR region.

No	Sample ID	Grain Size Fractions (µm)		Absorption Features (µm)	
		Calcite	Dolomite	Position 1	Position 2
1	II-CD.01	< 45	125-500	2.33686	2.53497
2	II-CD.02	45-125	45-125	2.33067	2.53188
3	II-CD.03	125-500	< 45	2.32448	2.5164
4	II-CD.04	< 45	45-125	2.32912	2.53033
5	II-CD.05	45-125	< 45	2.33221	2.53188
6	II-CD.06	< 45	< 45	2.33067	2.53033
7	II-CD.07	45-125	125-500	2.32912	2.52723
8	II-CD.08	125-500	45-125	2.32757	2.52259
9	II-CD.09	125-500	125-500	2.32912	2.52569

Appendix VIII

Absorption features as a function of the weight percentage of the calcite in the synthetic samples

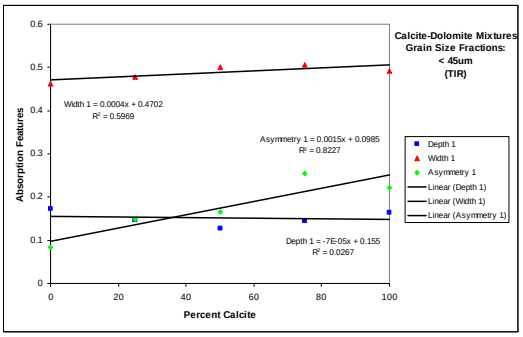

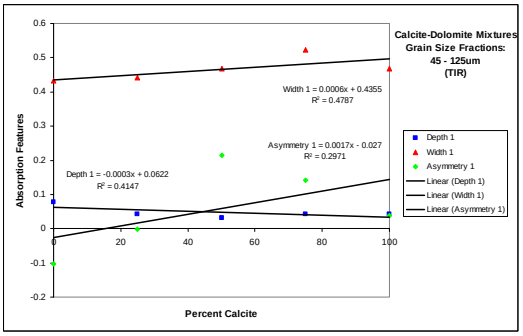

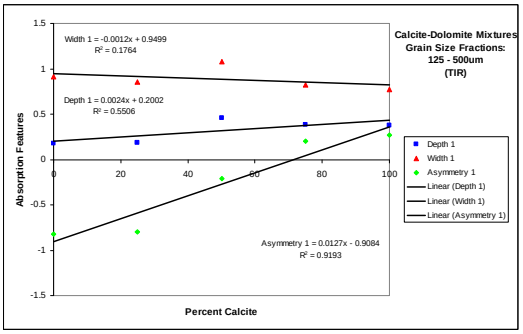

The positions of absorption features of the calcite-dolomite mixture with different grain size fractions and the same weight percentage of the carbonate mineral contents in the TIR region.

No	Sample ID	Grain Size Fractions (µm)		Absorption Features (µm)	
		Calcite	Dolomite	Position 1	Position 2
1	II-CD.01	< 45	125-500	11.4561	14.0058
2	II-CD.02	45-125	45-125	11.4687	13.9411
3	II-CD.03	125-500	< 45	11.4135	13.6478
4	II-CD.04	< 45	45-125	11.4577	13.99
5	II-CD.05	45-125	< 45	11.4151	13.6841
6	II-CD.06	< 45	< 45	11.453	13.9774
7	II-CD.07	45-125	125-500	11.4719	13.9805
8	II-CD.08	125-500	45-125	11.4277	13.6683
9	II-CD.09	125-500	125-500	11.7037	13.9175

Appendix IX

The position of absorption band of the rock samples from the transect 1 of the Bédarieux dolomite mine and the synthetic samples of the dolomite with different grain size fractions and the same packing model (model 1) in the SWIR region.

Rock Sample		Synthetic Sample (Pure Dolomite)	
Sample ID	**Position 1 (µm)**	**Grain Size Fraction (µm)**	**Position 1 (µm)**
BMP14	2.32138	< 45	2.32293
BMP15	2.32138	45-90	2.32293
BMP16	2.32138	90-125	2.32293
BMP17	2.32138	125-250	2.32138
BMP18	2.32293	250-500	2.32138
BMP19	2.32138	> 500	2.32138
BMP20	2.32138	-	-
BMP21	2.32138	-	-

The position of absorption band of the rock samples from the transect 2 of the Bédarieux dolomite mine and the synthetic samples of the pure moura calcite marble and chemical pure dolomite mixtures with grain size fractions 125-500µm and the same packing model (model 1) in the SWIR.

Rock Sample		Synthetic Sample	
Sample ID	**Position (µm)**	**Percent Dolomite**	**Position (µm)**
BMP22	2.32138	0	2.33995
BMP23	2.32138	25	2.33531
BMP24	2.31983	50	2.32912
BMP25-a	2.33686	75	2.32448
BMP25-b	2.32293	100	2.32138
BMP26	2.32138	-	-
BMP27	2.31983	-	-
BMP28	2.31983	-	-
BMP29	2.32138	-	-

Appendix X

Position of absorption band of rock sample spectra derived from laboratory and HyMap2003 spectra of the position of the carbonate absorption feature from the rock samples collected in the two transect of the Bedarieux dolomite mine.

Transect 1

Sample ID	Laboratory Feature	HyMap Feature
	Position 1	Position 1
14	2.32138	2.3090
15	2.32138	2.3090
16	2.32138	2.2920
17	2.32138	2.2920
18	2.32293	2.3090
19	2.32138	2.3090
20	2.32138	2.3090
21	2.32138	2.3090

Transect 2

Sample ID	Laboratory Feature	HyMap Feature
	Position 1	Position 1
22	2.32138	2.3090
23	2.32138	2.3090
24	2.32138	2.3090
25-a	2.33686	2.3090
26	2.32138	2.3090
27	2.32138	2.3090
28	2.32138	2.2920
29	2.32138	2.3090